Max-Planck-Institut für Meteorologie
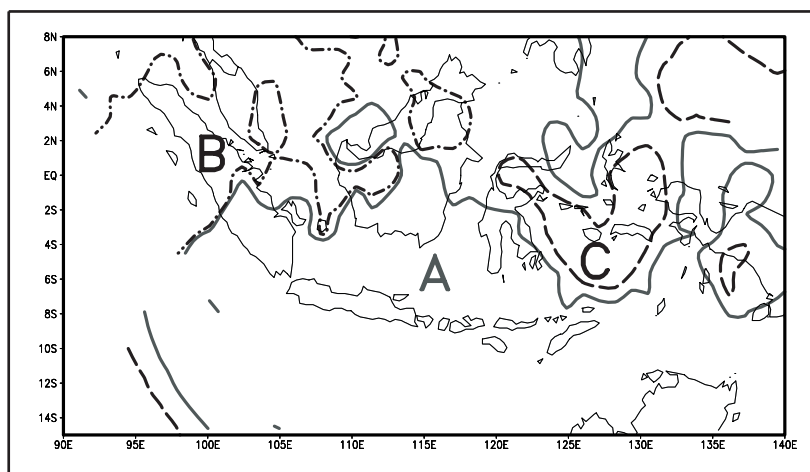*Max Planck Institute for Meteorology*

Report No. 346

Variability of Indonesian Rainfall and the Influence of ENSO and Resolution in ECHAM4 Simulations and in the Reanalyses

by

Edvin Aldrian · Lydia Dümenil Gates · F. Heru Widodo

Authors

Edvin Aldrian

Max-Planck-Institut für Meteorologie
Hamburg, Germany
&
Agency for the Assessment and
Application of Technology
Jakarta, Indonesia

Lydia Dümenil Gates

Lawrence Berkeley National Laboratory
Berkeley, CA, USA

F. Heru Widodo

Agency for the Assessment and
Application of Technology
Jakarta, Indonesia

Max-Planck-Institut für Meteorologie
Bundesstrasse 55
D - 20146 Hamburg
Germany

Tel.:   +49-(0)40-4 11 73-0
Fax: +49-(0)40-4 11 73-298
e-mail: <name>@dkrz.de
Web: www.mpimet.mpg.de

Variability of Indonesian Rainfall and the Influence of ENSO and Resolution in ECHAM4 Simulations and in the Reanalyses

Abstract

A study on the skill of the atmospheric general circulation model ECHAM version 4 and two reanalyses in simulating the Indonesian rainfall is presented with comparisons to 30 years of rain gauge data. The reanalyses are those performed by the European Centre for Medium-Range Weather Forecasts and of the National Centers for Environmental Prediction jointly with National Center for Atmospheric Research. This study investigates the skill of the reanalyses and ECHAM4 with regard to regional, annual and interannual variability of rainfall and its responses to El Niño-Southern Oscillation (ENSO) events. The study is conducted at two resolutions, T42 and T106.

A new regionalization method called the double correlation method is introduced. With this method, the Maritime Continent is divided into three climate regions, the south monsoonal, the northwest semi-monsoonal and the Molucca anti-monsoonal region. Except over Molucca, the reanalyses and ECHAM4 simulate these annual rainfall patterns quite well.

The three regions are used to study the variability of Indonesian rainfall and to measure the skills of the reanalyses and ECHAM4. The skill of rainfall simulations in Indonesia depends on the region, month and season, and the distribution of land and sea. Higher simulation skills are confined to years with ENSO events. Except for the region of northwest Indonesia, the rainfall from June (Molucca) and July (south Indonesia) to November is influenced by ENSO, and it is more sensitive to El Niño than La Niña events. The observations show that the Moluccan region is more sensitive to ENSO, receives a longer ENSO impact and receives the earliest ENSO impact in June. The ENSO impact will diminish in December. It is found that the reanalyses and the climate model simulate the seasonal variability better than the monthly one. The seasonal skill is the highest in June/July/August, followed by September/October/November, December/January/February and March/April/May. The correlations usually break down in April (for monthly analysis) or in spring (for seasonal analysis). In general the performance of ECHAM4 is poor, but in ENSO sensitive regions and during ENSO events, it is comparable to the reanalyses. The introduction of a higher resolution land-sea mask improves the model performance. Besides rainfall variability, signatures of the ENSO impact, the spring correlation breakdown and annual cycles are better represented by the higher resolution model.

1   Introduction

The Indonesian Maritime Continent is an interesting region for climate research. In atmospheric dynamics, this region is influenced by both the Hadley and Walker cells. The seasonal to interannual variabilities of Indonesian rainfall are characterized mainly by the monsoon (*Ramage*, 1971) and the El Niño-Southern Oscillation (ENSO; *Philander* 1989; *Ropelewski and Halpert* 1987, 1989; *Halpert and Ropelewski* 1992). Indonesia experiences two monsoons every year.

They are the wet monsoon from November until March, which coincides with the presence of the Inter-Tropical Convergence Zone (ITCZ) in this region (*Asnani*, 1993), and the dry monsoon from May until September, when the dry southeasterly wind blows from Australia. *Ramage* (1971) and *Cheang* (1987) mentioned April and October as the transitional months. Annual and interannual climate variability in Indonesia is quite unique, as it is not homogenous over the whole region (*Wyrtki*, 1956) and the coherence of rainfall patterns varies with the season (*Haylock and McBride*, 2001). ENSO contributes to the rainfall pattern in this area and its influence is interconnected with the monsoons (*Lau and Nath*, 2000). During El Niño (La Nina) events or warm (cold) phases, this region experiences lower (higher) rainfall than in other years (*Gutman et al.*, 2000). So far, discussions of Indonesian rainfall variability in relation to ENSO have used the Southern Oscillation index (SOI). For example *Braak* (1919); *Berlage* (1927); *Schell* (1947); *Reesinck* (1952) and later *Nicholls* (1981) reported a good correlation between rainfall variations in Indonesia and the SOI. Here, we will use another ENSO predictor, the NINO3 sea surface temperature (SST), which has been used by many ENSO forecasting groups (*Barnston et al.*, 1999).

Recent analyse extends to include atmospheric general circulation model (AGCM) simulations. *Goddard et al.* (2000) gave a comprehensive review of the seasonal and inter-annual skill of climate simulations over recent decades, including the performance of AGCMs in general. *Barnett et al.* (1997) did a predictability analysis of mid-latitude climate on ensembles of simulations with the ECHAM4 (*Roeckner et al.*, 1996a) and the NCEP atmospheric model and found that the models' skill is higher by about 50% during strong SST events in the tropical Pacific. *Moron et al.* (1998) examined the skill and reproducibility of seasonal rainfall in the tropics for the ECHAM4 model at resolution T30. They found that with regard to the June to September inter-annual variability over southeast Asia from Pakistan to Taiwan (including Indonesia), the skill of ECHAM4 is mainly confined to years of strong tropical Pacific SST variability. Nonetheless there is yet no specific study addressing the influence of higher resolution on the skill of a GCM in the region.

There have been many studies on the quality of the simulated rainfall for the National Centers for Environmental Prediction and National Center for Atmospheric Research (NCEP-NCAR) reanalysis (*Kalnay et al.*, 1996) and the ERA15 (*Gibson et al.*, 1997) from the European Centre for Medium-Range Weather Forecasts (ECMWF). *Janowiak et al.* (1998) found good agreement with regard to large scale features and substantial differences in regional precipitation between the NCEP reanalysis and observation from the Global Precipitation Climatology Project (GPCP; *WCRP* 1990). *Stendel and Arpe* (1997) found that ERA15 precipitation fields were superior in the extra tropics to other reanalyses when compared with GPCP data. *Annamalai et al.* (1999) found the ERA15 to be better than other reanalyses in describing the Asian summer monsoon, while *Newman et al.* (2000) point to a substantial problem with the precipitation in the warm pool area near the Maritime Continent by all reanalyses.

The purpose of this study is an assessment of the performance or skill of the two reanalyses and the Max-Planck-Institute's atmospheric model ECHAM4 in simulating the variability of Indonesian rainfall as documented by gauge observation and how their performances vary in regard to the monsoon, ENSO, ITCZ and model resolution. The study will focus on monthly and seasonal means, but will examine interannual aspects of rainfall. One of the problems in simulating the Indonesian rainfall is the land-sea representation. Most of the areas are highly complex with oceans and chains of islands, which are difficult to represent even by a high-resolution model. Thus, it is important to study the role of the model resolution. Due to the high level of heterogeneity in the region, it has to be speculated that the typical horizontal resolution used in GCMs cannot adequately represent the complex interactions of mountains, air and sea. We have therefore included a higher resolution simulation with the same model in order to determine the ECHAM resolution required to make useful simulations in the region and classified regions according to major climate controls using rain gauge data.

The outline of this paper is as follows. Section 2 discusses data and the ECHAM4 model, section 3 regional and annual climate cycle analyses, section 4 inter-annual variability and section 5 seasonal and monthly variability. In section 6 the relation of rainfall variability to ENSO is investigated while section 7 discusses the land-sea mask effect at different resolutions. Finally, section 8 presents conclusions.

2   Data and Model

The data used in this study are monthly rainfall data collected by the Indonesian Meteorological & Geophysical Agency (BMG) at 526 stations all over Indonesia, and monthly mean rainfall data from the WMO-NOAA project on The Global Historical Climatology Network (GHCN; *Vose et al.* 1992) from 1961 to 1993. In our area of interest (15 °S - 8 °N and 95 °E - 145 °E), there are 884 rain gauges (Fig. 1). These data are gridded to match the other datasets at T42 and T106 resolutions.

This study uses two reanalysis data sets. The first is ERA15 (*Gibson et al.*, 1997), which is available at the horizontal resolutions of T42 and T106 (the original calculation) or equivalent to 2.8125 ° and 1.125 ° in the tropics, respectively, from 1979 until 1993. The second one is the 40 year NCEP reanalysis (NRA; *Kalnay et al.* 1996), from which the time period from 1961 to 1993 with a fixed spatial resolution of T62 (equivalent to 2.5 ° in the tropics) is used. For comparisons with other T42 products, a regridding procedure is applied to change the NRA grid format from T62 into T42.

The ECHAM4 (*Roeckner et al.*, 1996a) model is a spectral model with a triangular truncation at the wavenumbers 42 (T42) and 106 (T106). For the vertical representation a 19 level
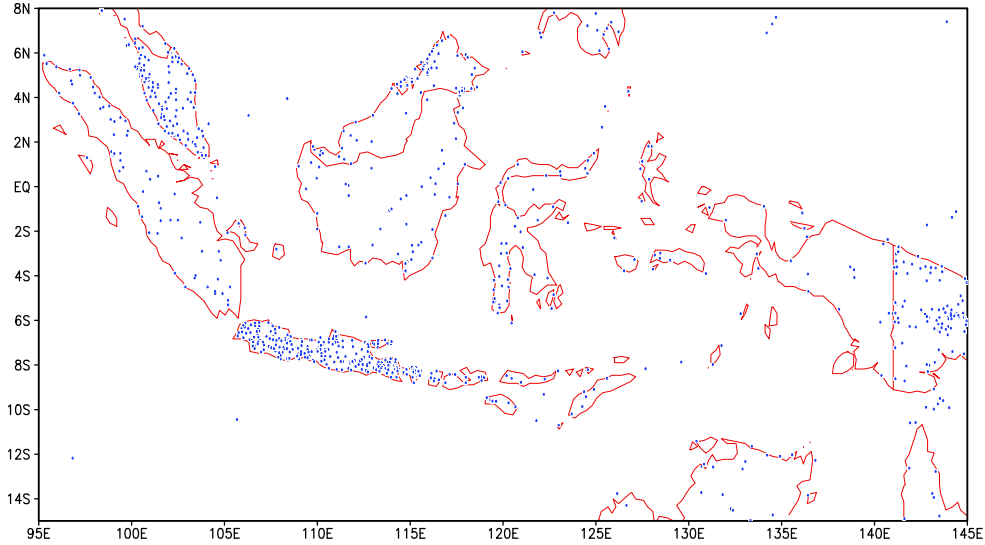
Figure 1: The distribution of rain gauge stations over the Indonesian archipelago or over 15S-8N, 95E - 145E with 884 stations.

hybrid sigma-pressure coordinate system is used. The time integration is carried out using a semi-implicit "leap-frog" method. The orography and the land-sea mask are calculated from a high resolution (1 km) US Navy data set. Unfortunately, due to limited computer resources, the T106 output is available only for 10 years from 1979 - 1988, while the coarser resolution (T42) is available from 1979 - 1993 (see Table 1). The ECHAM4 model was driven by interannually varying SSTs from the Atmospheric Model Intercomparison Project 2 (*Gates*, 1992; *Gates et al.*, 1999) at both resolutions.

In addition, SST data from the GISST2 (Global Ice and Sea Surface Temperature) dataset (*Rayner et al.*, 1996) are used. This dataset is compiled from SST observations from 1903 - 1994 with a spatial resolution of 2.50, and is used to determine the ENSO years. The resolution of this data set is not of main concern here, because only an area average on NINO3 (50 $^{\circ}$S - 50 $^{\circ}$N, 150 $^{\circ}$W - 90 $^{\circ}$W) is taken into account. With the definition of an ENSO year by (*Roeckner et al.*, 1996b), SST anomalies are classified as an ENSO event if they are larger than 1 $^{\circ}$K in

Table 1: Resolutions and time span of data sets used

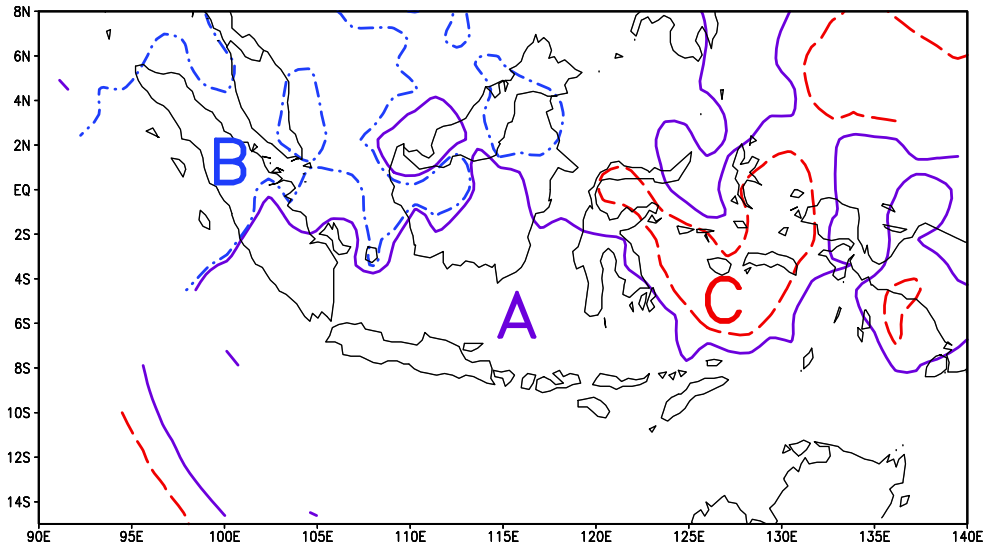|	Resolution	Time span
Rain gauge data	T42 / T106	1961 1993
ERA15	T42 / T106	1979 1993
NRA	T42 (regridded from T62)	1961 1993
ECHAM4	T42 / T106	T42: 1979 1993;
		T106: 1979 1988

Figure 2: Three climate regions using the double correlation method, which divides Indonesia into region A (solid curve); the southern monsoonal region, region B (dashed-dotted curve); the semi-monsoonal region and region C (long dashed curve); the anti monsoonal region.

amplitude and persist for more than one year in the NINO3 region. As a result, the ENSO years from 1961 - 1993 are as follows:

El Niño year: 1965, 1969, 1972, 1982, 1987, and 1991

La Niña year: 1964, 1970, 1973, 1975, and 1988

3 Regional Annual Cycle Analysis

Due to a high horizontal variability in this region (*Haylock and McBride*, 2001), there is a need to classify regions according to their annual rainfall cycles. The first regionalization attempt was made by *Wyrtki* (1956), when he divided the Indonesian waters into nine subregions. Here we introduce the double correlation method in which it is noted that grid cells with similar annual cycles are likely to respond similarly and homogeneously to a climate phenomenon and shall belong to a region. Each of the regions must be distinct from the others and each is influenced by the specific dominant climate phenomenon acting on it. To establish a strong climate pattern, this section utilizes long term observations from 1961-1993.

With the double correlation method, we look for a region, in which the annual cycles of its grid cells are correlated among themselves above a certain threshold value. For higher efficiency, rather than correlating all grid cells to each other, we first select some reference cells. Secondly we correlate all other cells to these reference cells based on their annual cycles. Cells that are
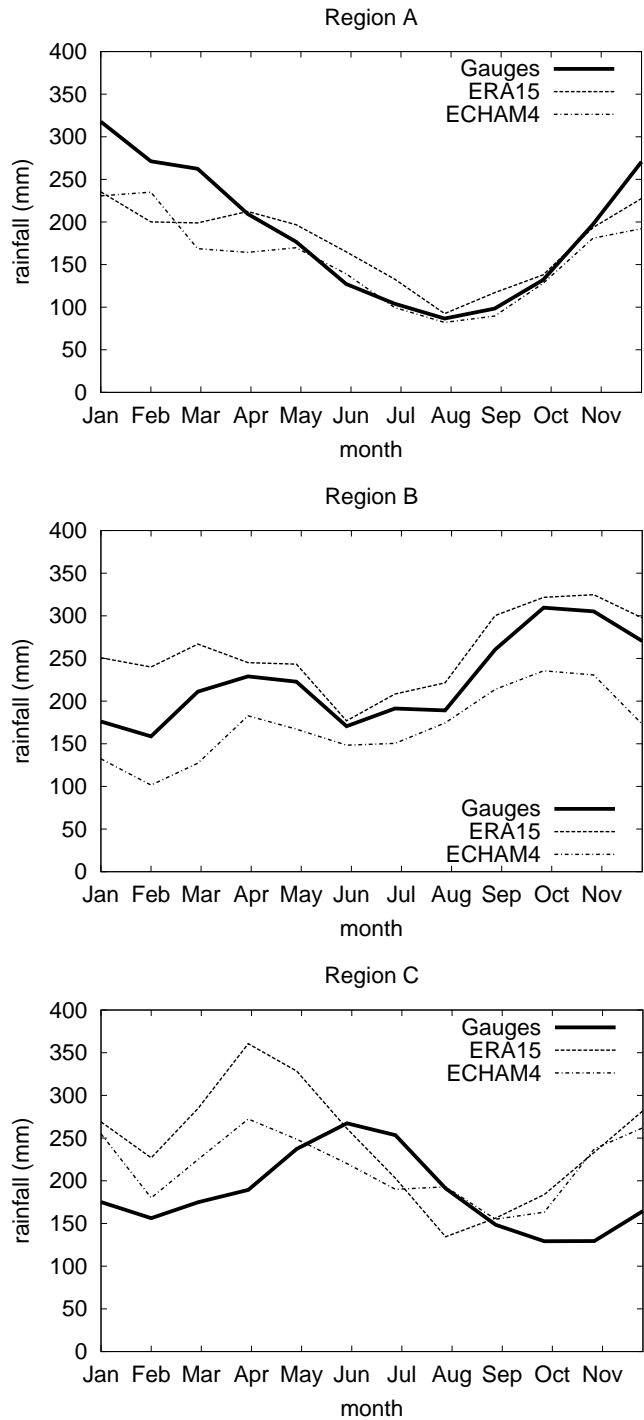
Figure 3: The annual rainfall cycle (mm/month) of each region at T106 resolution for observation with rain gauge (bold), ERA15 (thin dashed) and the ECHAM4 simulation (thin dot-dashed).

correlated above a certain threshold value are belonging to a region. Thirdly we correlate all grid cells again with the mean annual cycle of the resulting region using the same threshold value. The aim of the second correlation is to produce a region independent of the choice of the reference grid. The threshold value should be the highest correlation value that produces no overlapping boundaries. In this paper the threshold value chosen is 0.67, which is the 99% significance level in our data from only one correlation. Thus, with double correlations, the level of significance is much higher. The result of this method is illustrated in Fig. 2, where the Maritime Continent is divided into three climate regions, the southern Region A, the north-western Region B and the Moluccan Region C. From now on, all analysis will use these three regions.

In order to show the similarity of the approaches, the first two Principal Components (PC) of Empirical Orthogonal Function (EOF) analysis from monthly rainfall over 25 °S - 25 °N and 20 °E - 180 °E were also calculated (not shown). PC 1, which represents the annual pattern, has 30.08% of all the variances and shows Region C over Molucca. The areal extent of this region is similar to Region C of the present method. Additionally, PC 1 shows Regions A and B (the positive part). PC 2 with 8.09% of total variance also shows Region B and represents the semi-annual patterns such as the double peaks of Region B. Those two PCs only explain less than half of the total variance because we took the whole dataset of 33 years. Other PCs explain non-annual patterns, while we are aiming only at the annual patterns for our regionalization.

The annual cycle given by observed data at T106 resolution in Region A is shown in Fig. 3. We observe maximum in December/January/February (DJF) and a minimum in July/August/September (JAS). This illustrates two monsoon regimes: the wet northeast monsoon from November to March (NDJFM) and the dry southeast monsoon from May to September (MJJAS). With a strong monsoonal cycle and the southern location, we refer to this region as the southern monsoonal region. The annual cycle of Region B has two peaks, in October/November/December (OND) and March/April/May (MAM). The peaks in OND and in MAM represent the southward and northward movements of the ITCZ respectively. *Davidson et al.* (1984) and *Davidson* (1984) described in detail the ITCZ movement in this region in boreal winter. We thus call Region B the northwest semi-monsoonal region. We also note in Fig. 3 that Region C is quite different from the others and has a peak in May/June/July (MJJ), and we therefore refer to this region as the Molucca anti-monsoonal region.

Along with the annual cycle from observations, Fig. 3 shows the annual cycle of ERA15 and ECHAM4 at T106 resolution over corresponding regions of Fig. 2. Patterns in Region A of ECHAM4 and ERA15 agree well with observations although the peaks of the wet season are less than observed. It is interesting to note that in Region A ERA15 and ECHAM4 show a very similar annual march. In Region B, ERA15 produces more rainfall than observations throughout the year in contrast to less rainfall given by ECHAM4. However, their correlations with regard to time with observations are above 0.80, which means that the representation of the annual
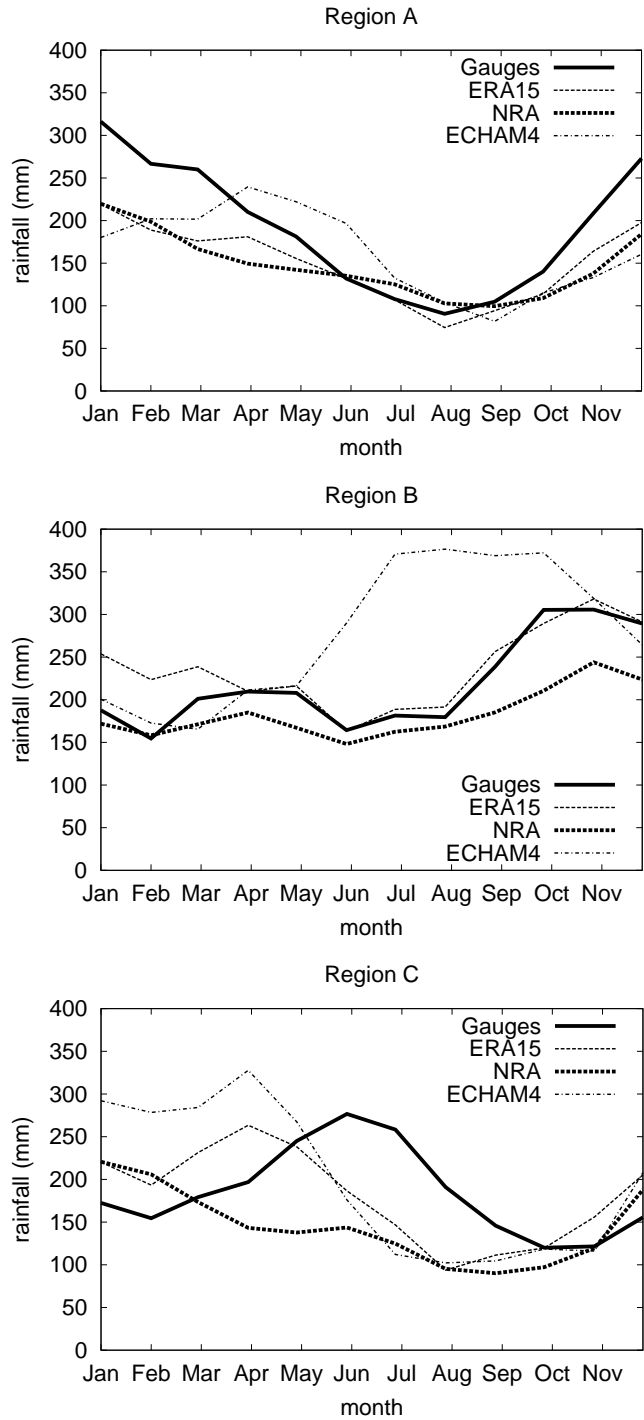
7

Figure 4: As Fig. 3, but for the T42 resolution, and NRA (bold dashed).

Table 2: Correlations of ERA15, NRA and ECHAM4 in three regions with the observed annual cycles. One, two and three asterisks indicate correlations at 90%, 99% and 99.9% significance levels, respectively.

| | Region A | | | Region B | | | Region C | | |
	Obs - ERA15	Obs - NRA	Obs - ECHAM	Obs - ERA15	Obs - NRA	Obs - ECHAM	Obs - ERA15	Obs - NRA	Obs - ECHAM
T42	0.97***	0.94***	0.56**	0.86***	0.97***	0.32*	0.27	0.01	0.13
T106	0.91***	-	0.93***	0.88***	-	0.88***	0.27	-	0.2

cycle is excellent. In Region C, the performances differ considerably. There the annual peak of ERA15 and ECHAM4 is found in MAM instead of in MJJ, and there is a strong overestimation of December rainfall. It is possible that these peaks represent an erroneous movement of the ITCZ.

At T42 resolution (Fig. 4) the reanalyses and model behave differently. In Region A, the reanalyses agree well and follow the observed annual cycle and they are particularly good in JAS, but again underestimate the wet DJF. ECHAM4 has a peak in MAM instead of NDJ and extends the wet season far too long into May and June. In Region B, ECHAM4 considerably overestimates rainfall from June to October i.e. during the dry period. In this region ERA shows an almost perfect annual cycle. NRA has a similar annual cycle as ERA15 but underestimates the peak in OND. In Region C, ECHAM4 and ERA15 again misplace the peak observed in June and July. The worst correlation in Region C is that of NRA, which is considerably different from to observations. In fact, NRA's annual cycle is similar to that in Region A. Table 2 summarizes the reanalyses and model skills with regard to their annual cycles. The reanalyses simulate temporal patterns of Region A and B quite well, while ECHAM4 shows large errors in Region B. However, neither reanalyses nor model show good agreement in Region C.

In summary of Fig. 3 and 4, NRA has a poorly pronounced annual cycle with no clear peak. NRA was produced at T62 and was truncated to T42, so should have the benefit of a higher resolution land-sea mask. Obviously, this information is not passed on to the atmosphere. In Region C ERA15 has a clear peak at both resolutions, but it occurs too early in the year. ERA15 at a coarser resolution has a less pronounced annual cycle. The performance of ECHAM4 at higher resolution resembles that of ERA15, although less pronounced, while ECHAM4 at lower T42 resolution disagrees with observations in all three regions.

This analysis can be used to explain correlation values in Table 2 or the deviations of their annual cycles in Fig. 3. Fig. 5 shows the regionalization that would result from ERA15 and ECHAM4 at T106 using the corresponding annual cycle procedure as in observations (Fig. 3).
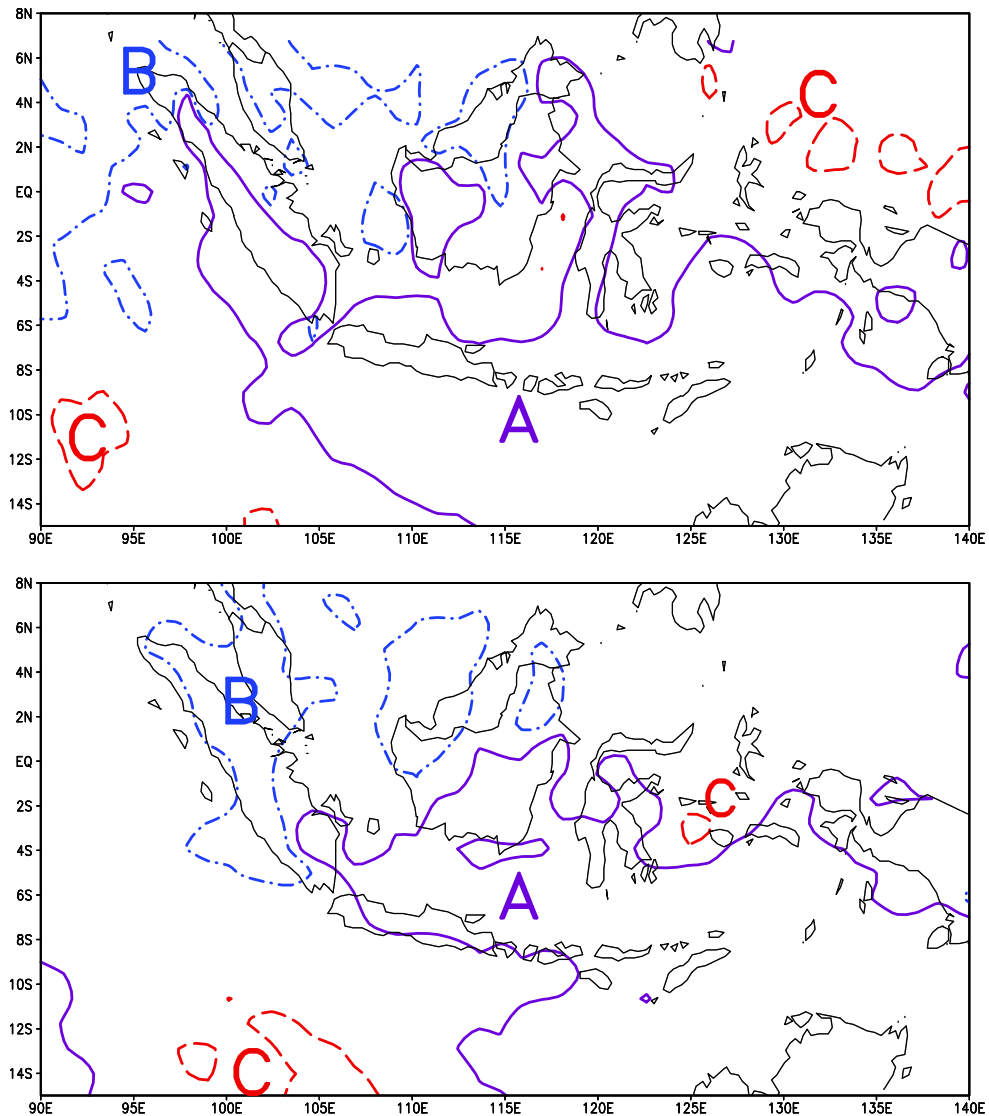
Figure 5: As Fig. 2, the climate regions at the T106 resolution as simulated by ERA15 (above) and ECHAM4 (bottom) using annual rainfall patterns of gauges as shown in Fig. 3.

In Fig. 5 for both ERA15 and ECHAM4 Region A and B, as expected, are located in southern and northwestern Indonesia, respectively. Meanwhile the climate of Region C is not in the proper location in the ERA15 results. ECHAM4 represents Region C climate only for one grid cell in central Molucca plus some areas south of Indonesia. These results show that ERA15 and ECHAM4 cannot perform well with regard to Region C in the previous analysis. ECHAM4 gives a broader Region B while ERA15 gives a broader Region A, the latter indicating a wider dry area or area affected by the southeast monsoon and the former indicating a longer period of wet northeast monsoon. Another feature are broader intermediate regions in both cases. The expected annual cycle of the intermediate region will be a flat one with two small peaks. Similar analysis at T42 resolution (not shown here) can be used in explaining values in Table 2 and patterns in Fig. 4.

4 Interannual Variability

The analysis of interannual variability in this study is based on monthly and seasonal (three-monthly) averages for the three climate regions. Fig. 6 to 8 show interannual variations of seasonal means of rainfall for different seasons from observations from 1961 to 1993, two reanalyses and ECHAM4 at T42. Values represent the interannual variations of the rainfall after removing their averages and trends in units of a standard deviation (σ). In Fig. 6 for Region A there are good correlations between observations and NRA in JJA and SON. Except for a weak El Niño of 1969, El Niño years coincide with rainfall below $-\sigma$ in JJA and SON. In general, the two reanalyses and the model simulation have the worst skill in MAM and the best in JJA. During extreme El Niño events such as in 1982, all show good skills from JJA and simulate this event quite well ($< -\sigma$) as it extends to DJF, except ECHAM4 in DJF. In the case of the weak 1987 El Niño, all simulate the event only in JJA and SON. The impact of La Niña is not as clear as El Niño's and occurs only in SON. The La Niña events of 1964, 1970, 1973 and 1975 have clear signals in SON. In general, the impact of El Niño on Region A is greater than the impact of La Niña. *Chen and van den Dool* (1997) indicated significantly higher predictability during El Niño phases than during La Niña.

Fig. 7 shows similar information for Region B. Agreement between observed precipitation and reanalyses or ECHAM4 is low in all seasons. This region seems to show no El Niño effects on rainfall (*Ropelewski and Halpert*, 1987), unlike in Region A. Surprisingly, the peaks from observations in the spring (MAM) of El Niño year 1965 and La Niña years 1973 and 1988 are high. They may be connected to strong monsoon activities, as the ITCZ is leaving Indonesia during this time of year.

Fig. 8 illustrates the interannual variations for Region C. SON has the highest skill for reanalyses and ECHAM4. Like Region A, all have the worst skill in MAM. In SON, the variations during the El Niño events of 1982, 1987 and 1992 are well simulated by the reanalyses and the model. Like Region A, Region C receives strong El Niño impacts that last from JJA to DJF with smaller magnitudes. Smaller magnitudes imply that Region A is more sensitive to El Niño than Region C. Since the El Niño impact or rainfall reduction occurs during the peak of the rainy season, the impact will be less devastating than that of Region A, which receives the impact during the dry season.

In the case of La Niña years there is no consistent feature among models and observations. In La Niña years 1964 and 1970, Region A has larger values in SON than in JJA. However, in JJA of the same year the index is higher in Region C. In La Niña year 1970, the variation index of Region C is higher in SON. All models show the La Niña of 1988 (JJA and SON) quite well. Reanalyses show the decreases of this La Niña activity in SON over Region A and C. In summary, reanalyses and ECHAM4 behave in accordance with observations only during extreme
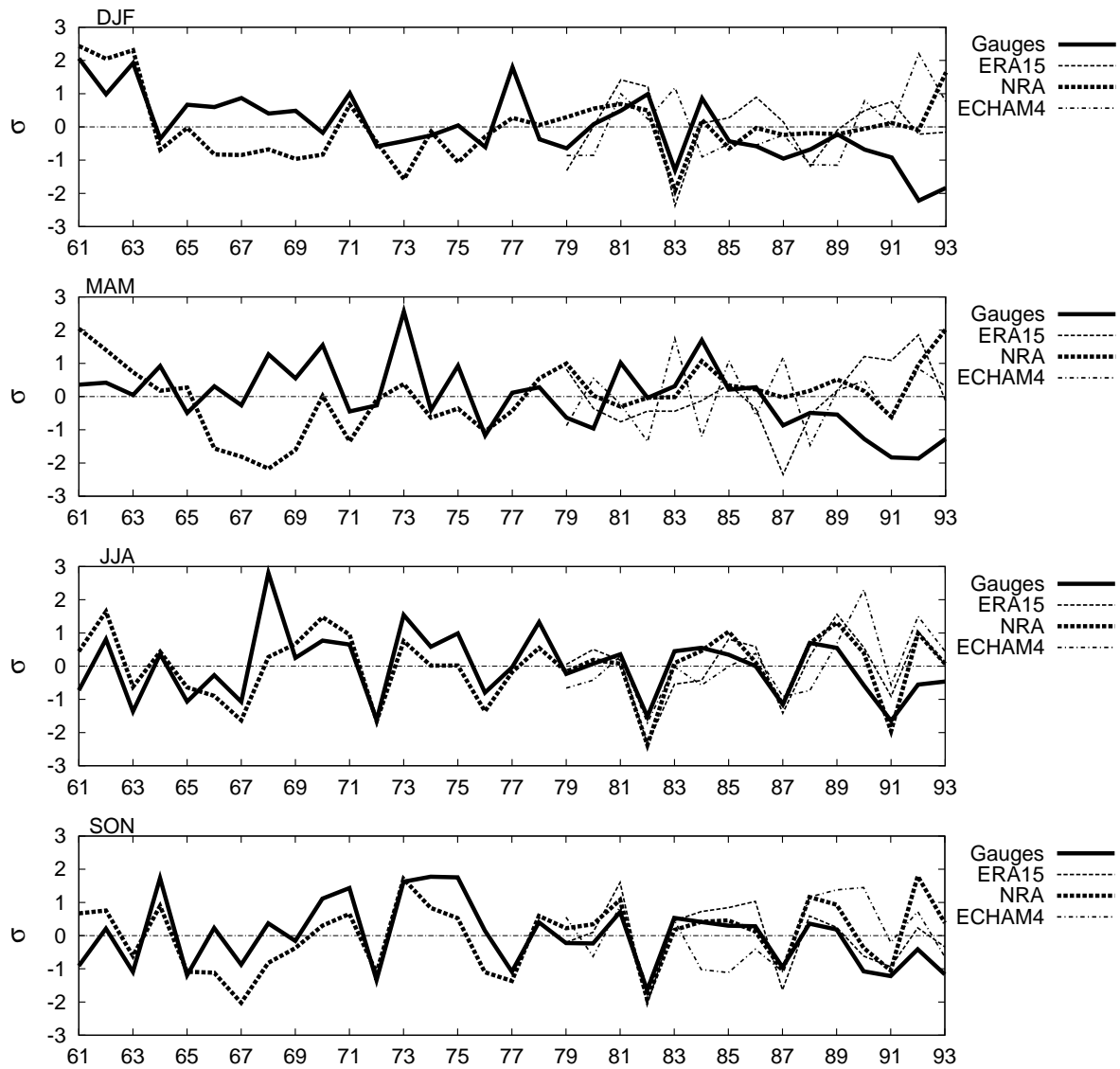
Figure 6: The inter-annual variation indices of seasonal rainfall in region A at T42 resolution for observation (bold solid), ERA15 (thin dashed), NRA (bold dashed) and ECHAM4 (thin dot-dashed). The ordinates are the variation of rainfall in units of standard deviation (σ).

12
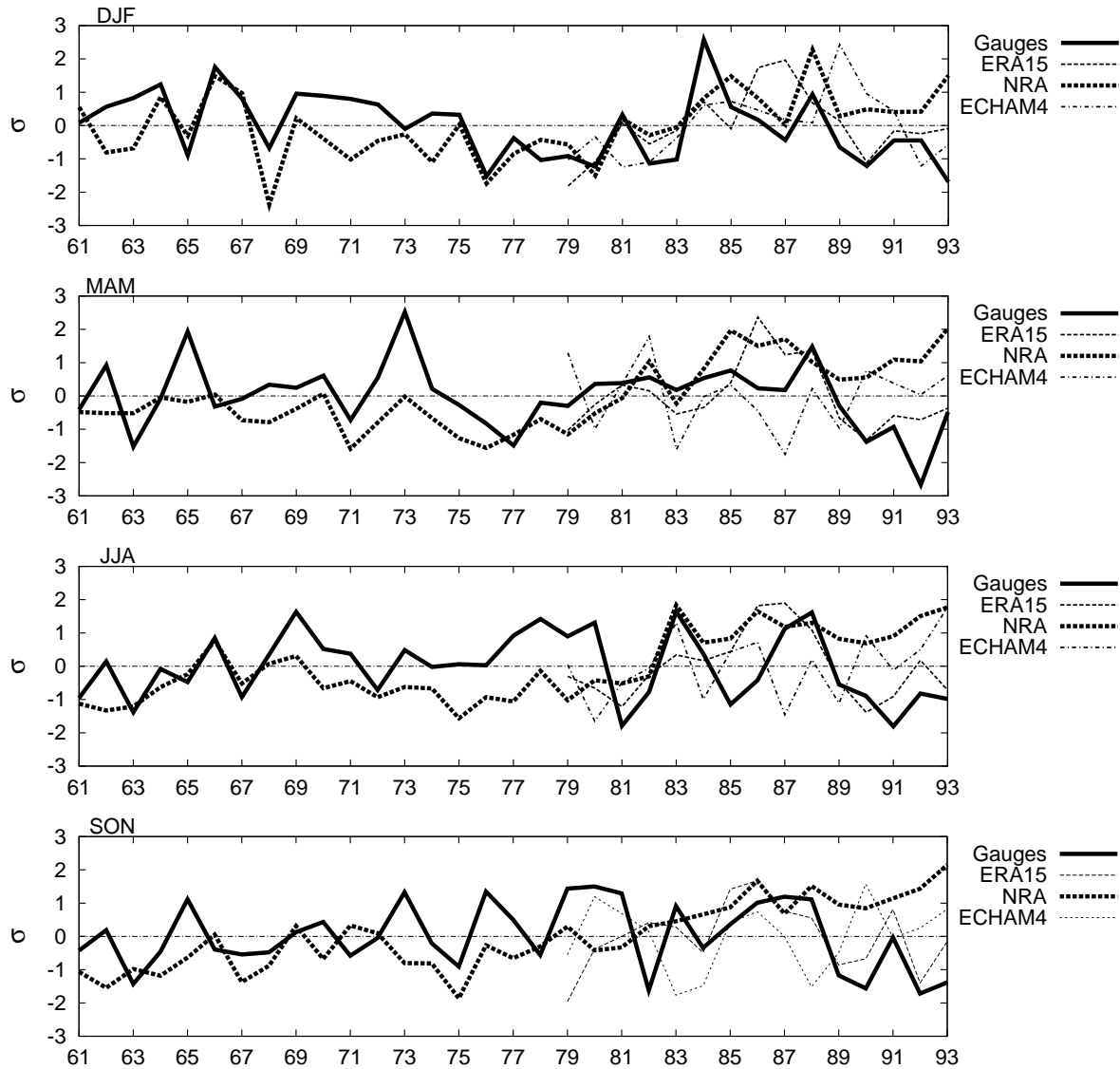
Figure 7: As Fig. 6, but for region B.

ENSO events. This agrees with the results of analysis of seasonal climate forecasts, which was found to be minimal in non-ENSO years (*Barnston et al.*, 1994; *Landman and Mason*, 1999). An example of a non-ENSO year, when the rainfall index is high in Regions A (JJA) and C (MAM and JJA) is 1984. The models do not simulate this well. The high rainfall index in this year is associated with a strong monsoon. Thus, models simulate variations due to ENSO events better than those due to monsoons.

Figure 8: As Fig. 6, but for region C.

5   Seasonal and Monthly Variability
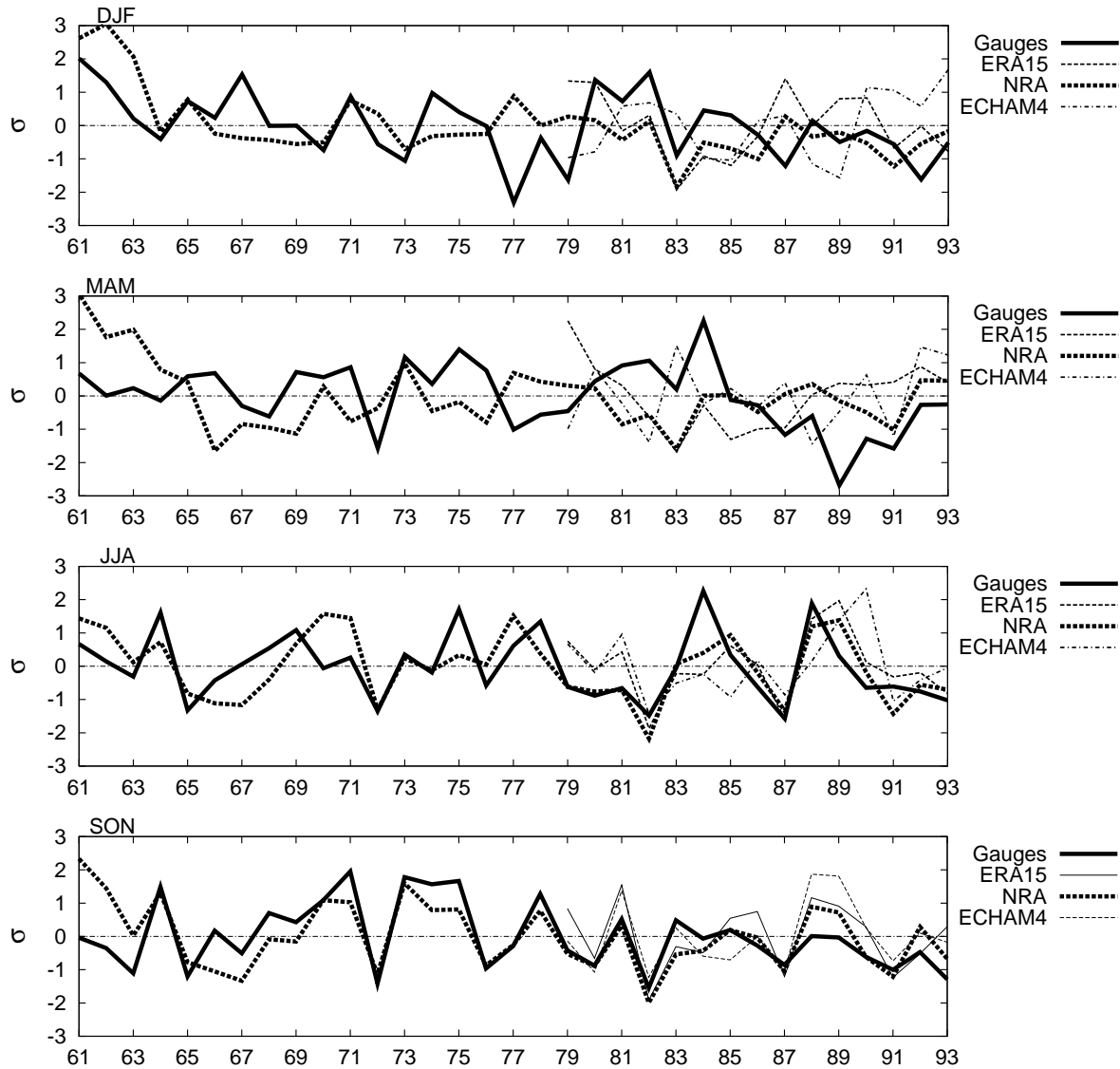
In Fig. 9 the seasonal mean correlations between observations and reanalyses and the model simulations, respectively, are compared for resolutions T42 and T106. Except for ECHAM4 at T106, which uses data from 1979-1988, correlations are calculated for data from 1979-1993. The measure of significant correlation is the 95% significance level.

Correlations show a distinct variation during the annual cycle. In Region A at T42, ECHAM4 has the same annual cycle variation as NRA. Only ERA15 shows a good correlation in DJF. Except for ECHAM4 in JJA in Region C, the correlations are significant in Region A and C for JJA and SON. In Region C the NRA reanalysis performs best. In Region A and C, the least insignificant correlation is in MAM and the highly significant one in JJA. There is a consistent

14

breakdown of correlations in spring in Regions A and C. In Region B NRA and ECHAM4 do not agree with the positive correlation of ERA15.

At the T106 resolution, the seasonal correlations of ERA15 and ECHAM4 in Region A are higher than those at T42. As at T42, the correlation breaks down in Regions A and C in the spring. Except for a low skill in DJF of ERA15 in Region C, the skill in Region A and C in general is similar to that at T42. In Region B, ERA15 at T106 has a similar feature and a better skill than at T42. As in the case of the annual cycle, the ECHAM4 performance in Region B is better for JJA at T106 than at T42. In Fig. 4 and 5, we saw that the annual cycle of ECHAM4 at T42 deviates significantly in JASO and higher resolution improves the annual cycle. Furthermore, there is a considerable improvement for ECHAM4 in the higher resolution in Region A and C in these seasons. In fact in JJA, ECHAM4 outperforms ERA15 in all regions. The inconsistent features in Region B in both resolutions suggest weak skill and low forcing by reanalyses and the ECHAM4 model.

Fig. 10 shows the monthly correlations of the T42 (left) and T106 (right) resolutions for the three regions. The variations from month to month are very high and do not retain the skill suggested before in seasonal mean analysis. In Region A at T42, the correlations of ECHAM4 are not in accordance with those of ERA15 and NRA, while the correlation of NRA agrees well with that of ERA15. In Region B at T42, again the correlation of NRA and ERA15 vary during the annual cycle in a similar way, but NRA has much smaller values. ECHAM4, on the other hand does not agree with either of them. In Region C at T42 the annual cycle of the correlations of the three are alike with the exception of ECHAM4 in August. NRA shows higher positive values while ERA and ECHAM4 agree at lower values most of the year. In Region A at T106 ECHAM4 agrees well with the monthly correlation of ERA15 except in JA and ON and with lower values. In Region B at T106 ECHAM4 resembles ERA15, but with smaller values. Again in Region C ECHAM4 is in phase with the variation of ERA15 except in August. The model shows yet again, as detected in the seasonal analysis of Regions A and C, the spring breakdown with the lowest correlations from February to April.

6   Interannual Variability Related to ENSO

From the above discussions, the impact of ENSO events is prominent in Regions A and C, that is, over most of Indonesia. *Nicholls* (1984) showed strong seasonal relations between SST in Indonesian waters and over the Pacific. Before that, *Nicholls* (1981) showed evidence of air sea interactions in Indonesia and that Indonesian rainfall is related to SST anomalies. Using the Southern Oscillation Index (SOI), an index based on the difference of mean sea level (MSL) pressure over Darwin and Tahiti, *Ropelewski and Halpert* (1989) showed that in an ensemble ENSO year annual variations of rainfall patterns in Indonesia (except in northwest

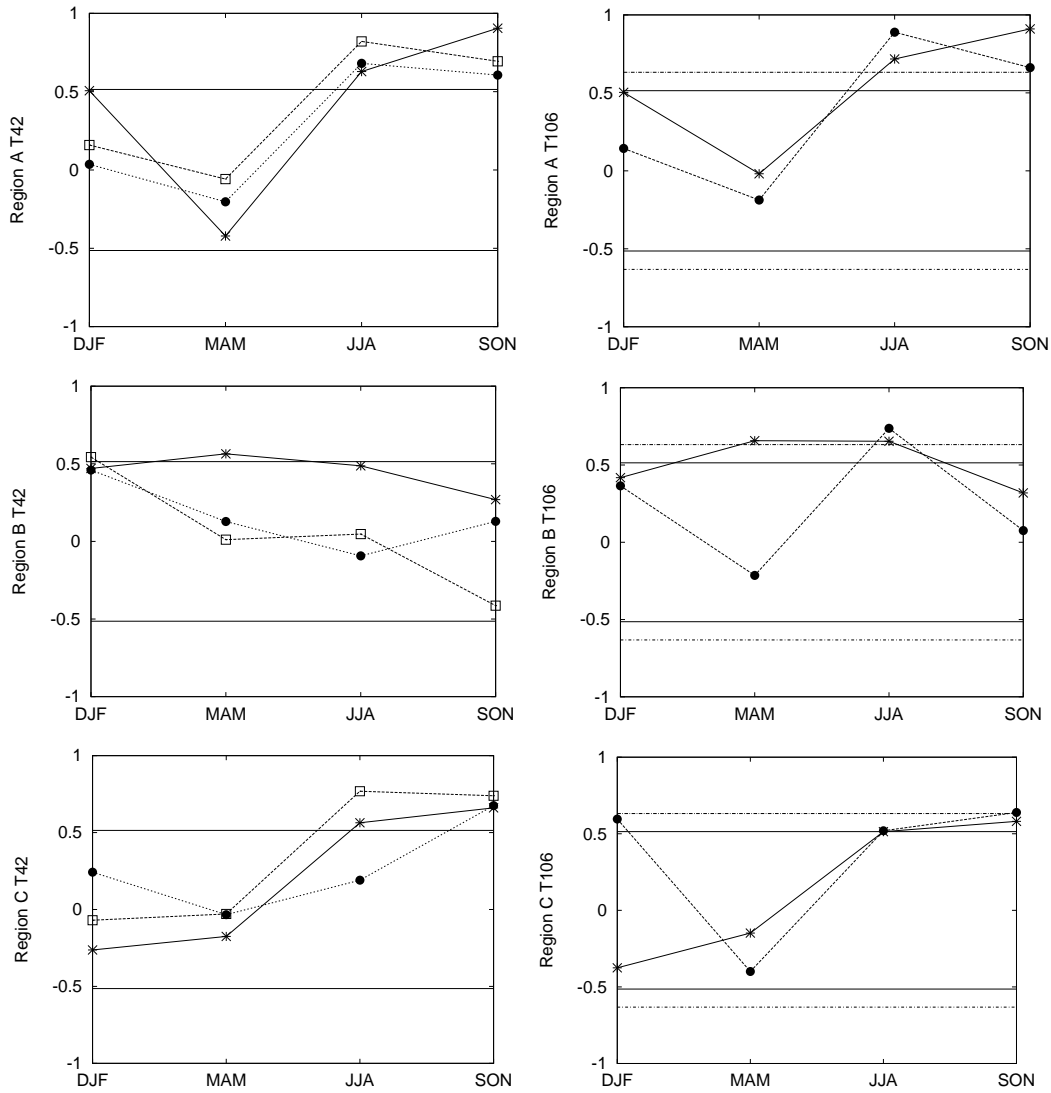Figure 9: The average seasonal correlation in region A (above), region B (middle) and region C (bottom) at T42 resolution (left) and at T106 resolution (right) between observation and ERA15 (∗), NRA (□) and ECHAM4 (●). Solid horizontal lines represent 95% significance levels on two sides for all data except ECHAM4 at T106; dashed horizontal lines represent 95% significance levels on two sides of ECHAM4 at T106.
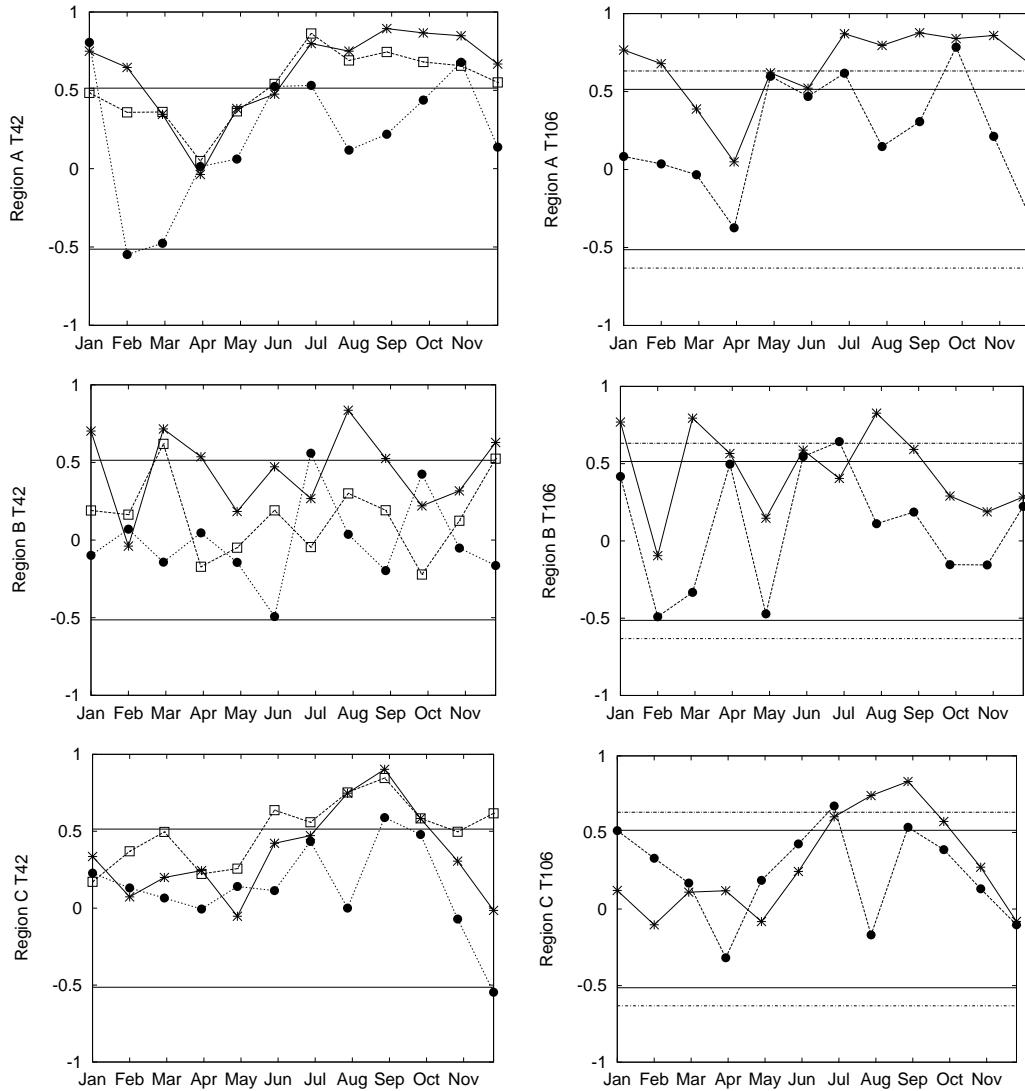
Figure 10: As Fig. 9, but for the average monthly correlation.

Indonesia) are 89% in coherence with SOI from 1885-1983, and that annual rainfall variations over Indonesia are associated with SST anomalies at 91% coherence during July of ENSO event years until June of the following year. *Ropelewski and Halpert* (1987) calculated that in Indonesia (except the northwestern part) during the period of June - November there is a coherence of interannual variation of rainfall with SOI of 82%.

ENSO events characterize the seasonal and monthly skills of the reanalyses and the ECHAM4 simulation. During ENSO years, reanalyses, the model simulation and observations show good agreement, especially in JJA and SON. Our results confirm that ENSO is the main driving force of high skill, which is in agreement with *Barnston et al.* (1994) and *Landman and Mason* (1999). From Fig. 6 and 8, ECHAM4 variability agrees with observations strongly only during ENSO events. However, the high predictive skill of ENSO impact is lost when the correlations in Region A and C break down in spring.
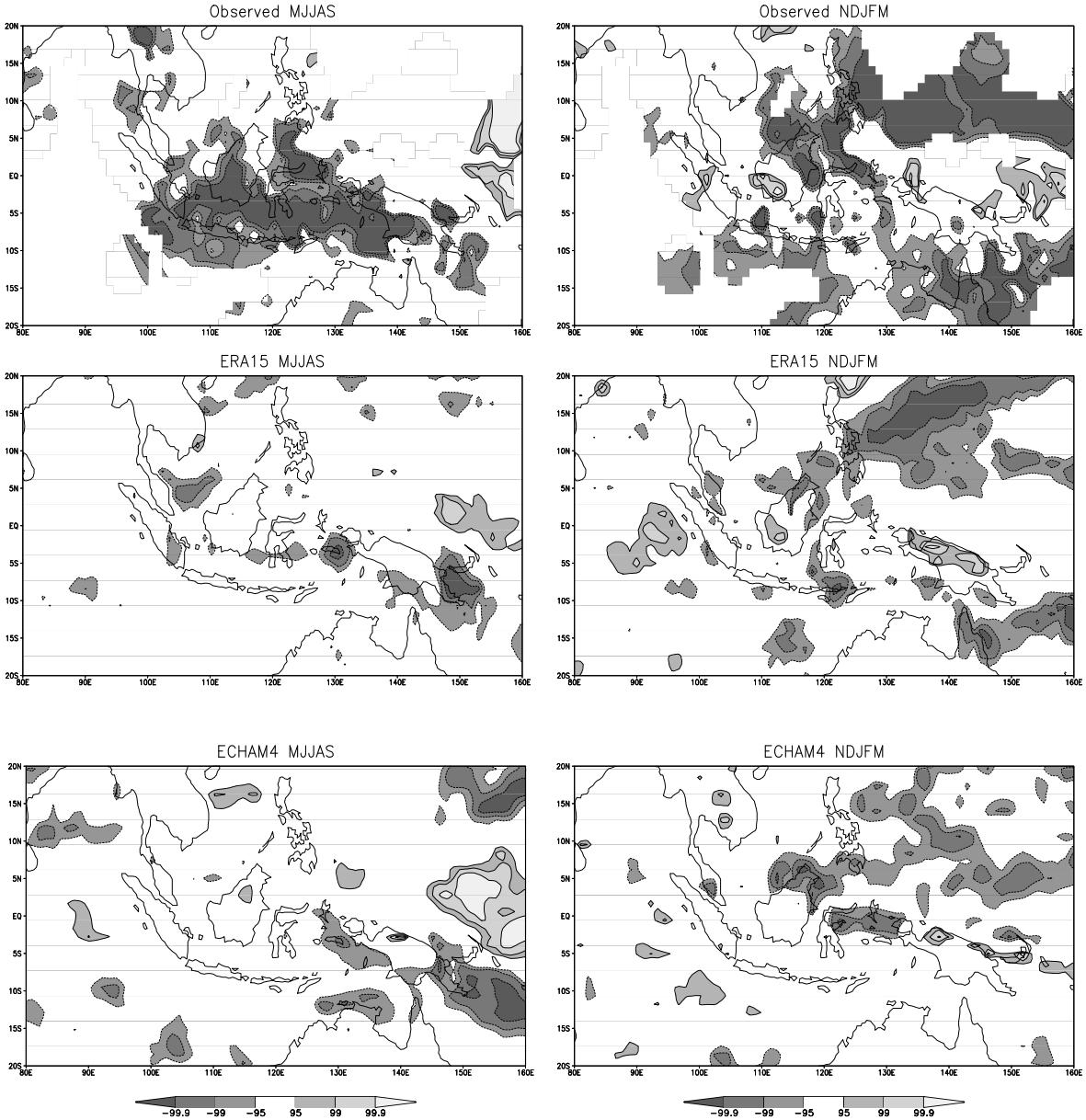
Figure 11: Spatial patterns of rainfall - NINO3 SST correlations for observations (top), ERA15 (middle) and ECHAM4 (bottom) during MJJAS (left) and NDJFM (right) at T106 resolution. All are shown with their statistically significant correlation level, where the solid (dashed) lines represent positive (negative) correlation. The three level of gray scales on both sides represent 95%, 99% and 99.9% significance levels. For example, for observed data (1961 - 1993), these significant levels correspond to correlation values |0.33|, |0.42| and |0.52| respectively.

6.1 Spatial Patterns of the Rainfall Sensitivity to NINO3 SST

Fig. 11 depicts the sensitivity of the Indonesian rainfall to NINO3 SST forcing during the dry monsoon (MJJAS) and the wet monsoon (NDJFM) (*Ramage*, 1971; *Cheang*, 1987). The sensitivity is indicated by the correlation between rainfall and NINO3 SST. This figure considers only correlation values with significance levels above 95%, 99% and 99.9%.

The impact of ENSO as defined by the observations is more prominent during MJJAS with a significant coherent area of negative signals in most parts of Indonesia. In NDJFM the observed rainfall data show significant negative responses to SST in south Indonesia, Molucca, northeast of Australia and a part of north Borneo. Some areas have good correlation values above 99% significance level in both seasons over 33 years (1961-1993). Region B does not have responses to NINO3 SST at all as shown by *Ropelewski and Halpert* (1987).

The ERA15 response in MJJAS is too weak and covers only a small area. In NDJFM, ERA15 shows good response over Kalimantan, north of the warm pool and south of New Guinea. ERA15 alsogives a significant positive response in west Sumatera in NDJFM. ECHAM4 shows too strong response in MJJAS east of 125E. In NDJFM, ECHAM4 gives a good response over Kalimantan, northern Molucca and north of the warm pool. For the remaining area,precipitation in ECHAM4 does not show a significant correlation to observations.

The exact period of ENSO impact on each region varies and needs further research on a seasonal or monthly basis. *Chen and van den Dool* (1997) and *Haylock and McBride* (2001) showed that the ENSO cycle predictability has a large seasonal dependence.

6.2 Seasonal and Monthly Variability Related to ENSO

Fig. 12 illustrates the negative seasonal mean correlation between rainfall and NINO3 SST for the three regions. A high correlation is indicated for T42 only in JJA for Region C for observations and in JJA and SON for Region A and C for ERA15. The two reanalyses follow the pattern for observations, especially in DJF, but are reduced to almost zero in MAM. In both these seasons, ECHAM4 gives erroneous positive correlations. The correlations between SST and precipitation for reanalyses and ECHAM4 follow highly observations in Regions A and C with strong negative values in JJA and SON. For ECHAM4, there are significant (above 99% correlation level) SST responses in SON (-0.51) in Region A, MAM (-0.52) in Region B and JJA (-0.47) and SON (-0.59) in Region C. In Region B correlations are insignificant indicating ENSO effect.

At T106 resolution, the positive role of a higher resolution becomes very clear in seasonal mean correlations of observations, ECHAM4 and ERA15. At this resolution, significant im-
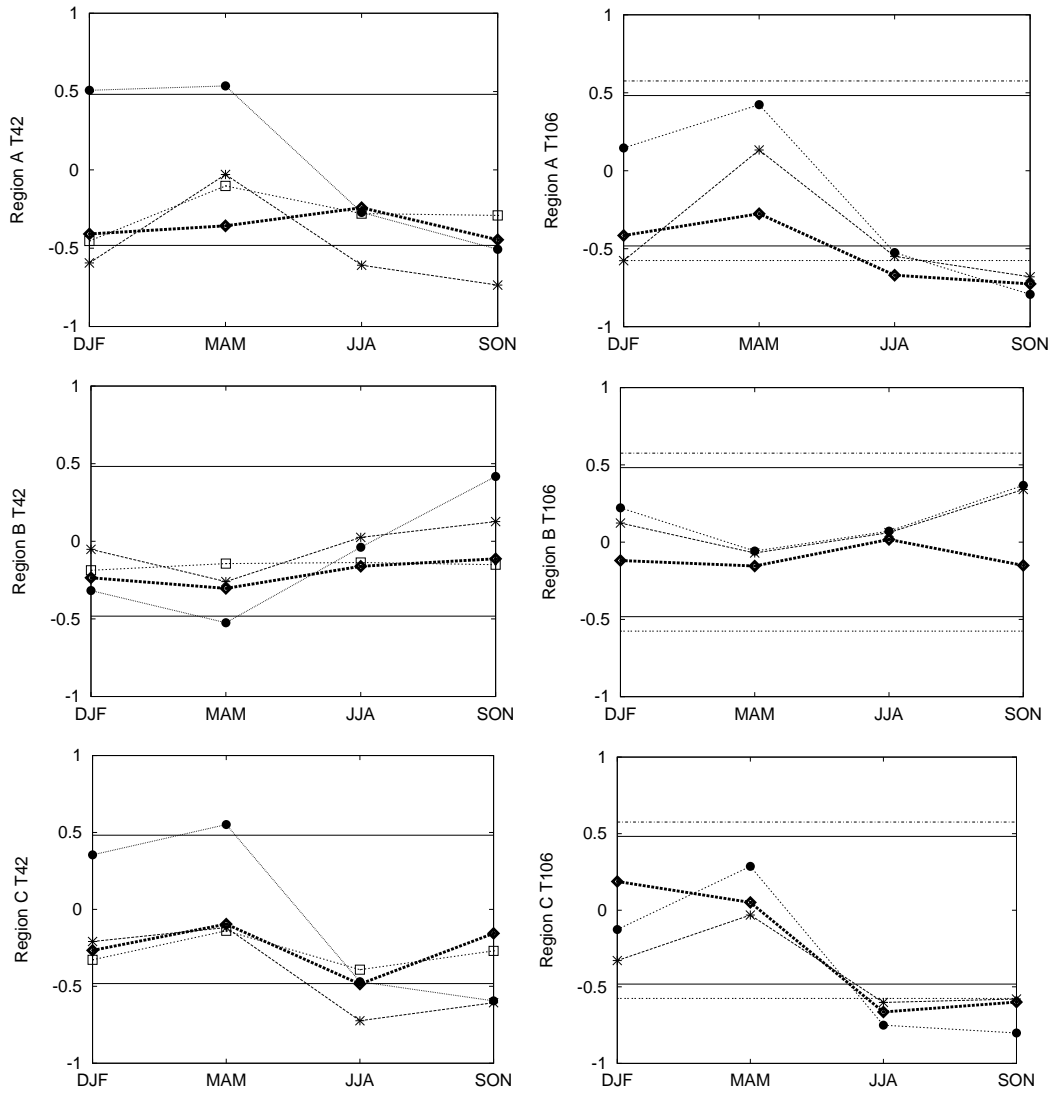
Figure 12: The seasonal mean values of correlations between NINO3 SST and average rainfall in region A (above), region B (middle) and region C (bottom) at the T42 resolution (left) and the T106 resolution (right) of observed data (◇), ERA15 (∗), NRA (□) and ECHAM4 (●). Solid horizontal lines represent 95% significant levels on two sides of all data except ECHAM4 at T106, while dashed horizontal lines represent 95% significant levels on two sides of ECHAM4 at T106.
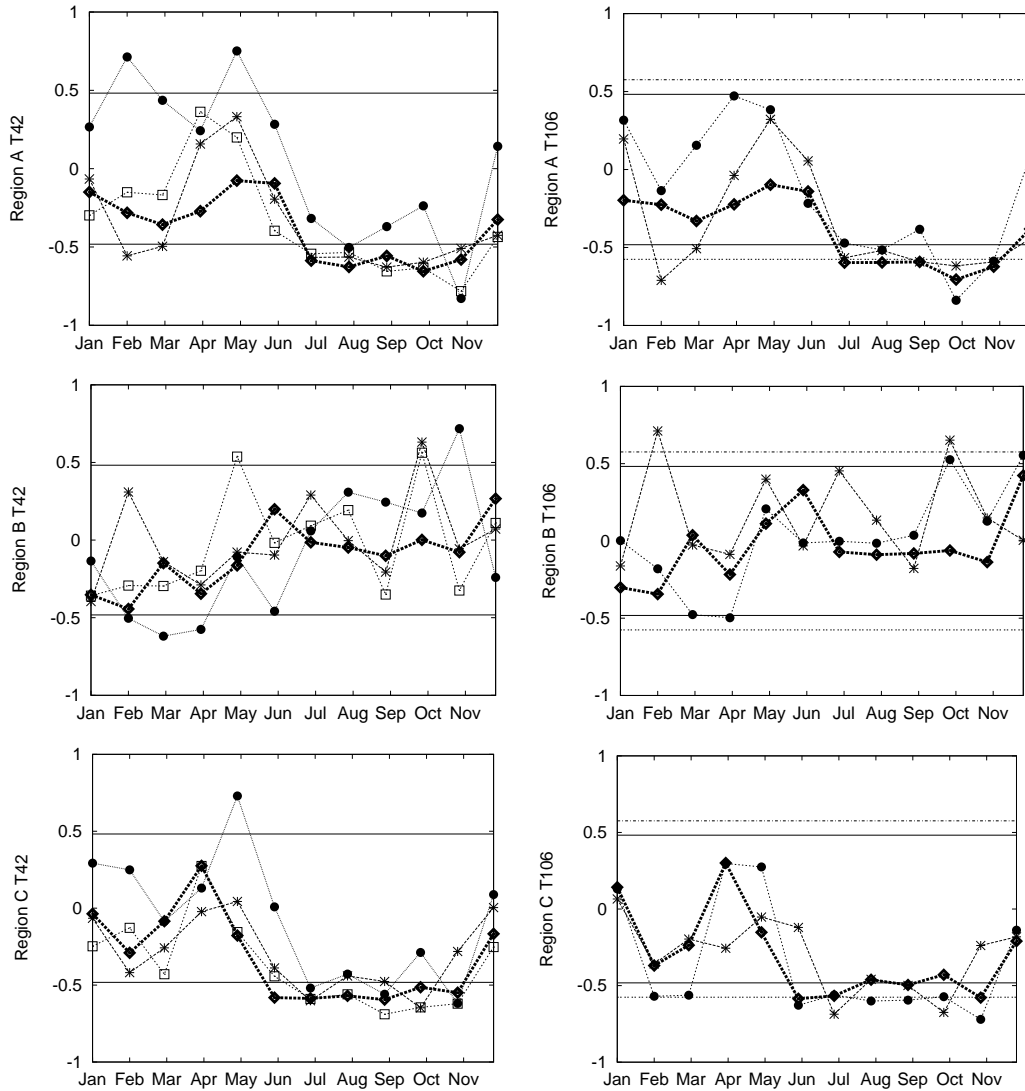
Figure 13: As Fig. 12, but for the monthly mean correlations.

provements of negative responses in JJA and SON, in agreement with observations, are seen
for Regions A and C. ECHAM4 performance is improved and the breakdown of correlations in
spring is even clearer with lower positive MAM values in Region C. Only in DJF and MAM for
Region A are the deviations of ECHAM4 responses higher than observations and reanalyses.
No significant values in Region B again confirm that this region shows no ENSO influence at
all. In Region B, ECHAM4 is very close to ERA15 and both have large errors compared to
observations in SON and DJF. Higher resolution only improves the model simulation in MAM.
A summary of seasonal rainfall response to SST variations at two different resolutions is given
in Table 3.

The correlations for monthly means similar to Fig. 12 are shown in Fig. 13. At T42, the
observations show more complicated structures and more significant correlations compared to
the seasonal analysis in Fig. 12. Correlations between observations are significant from July

Table 3: The seasonal correlation of rainfall with. NINO3 SST. One, two and three asterisks indicate the correlations at the 90%, 95% and 99% significance levels, respectively.

	Region A			Region B			Region C		
	Obs - ERA15	Obs - NRA	Obs - ECHAM	Obs - ERA15	Obs - NRA	Obs - ECHAM	Obs - ERA15	Obs - NRA	Obs - ECHAM
T42	0.16	0.26	-0.08	0.98***	0.19	0.97***	0.64*	0.90***	0.45
T106	0.81**	-	0.99***	-0.17	-	-0.22	0.82**	-	0.89***

to November in Region A and from June to November in Region C. In other words, the ENSO impact is significant in the dry period and the transition period to the wet period and ENSO has no impact on the peak of the wet northeast monsoon in DJF (Fig. 3). A significant response of rainfall in Region C on Nino3 SST in June indicates that this region receives an ENSO impact earlier than Region A, and the rainfall in June foreshadows the ENSO event. However, there is no clear improvement at the higher resolution. In both resolutions, the reanalyses and the model follow quite well the observed response between June and December in Regions A and C. The observed data show that the correlations at T42 are higher than at T106 in Region C. In spring, the correlation breaks down in Region A and C as before. The correlation values of ECHAM4 for both resolutions exhibit erroneously high values in Regions A and C in the spring. As before, the performance of ECHAM4 improves considerably for higher resolution. NRA and ECHAM in Region C have the best responses all year long, with correlation values of 0.88 with observations. In Region B, there is yet again no indication of an ENSO impact.

Table 4: The monthly correlation of rainfall vs NINO3 SST. One, two and three asterisks indicate correlation at the 95%, 99% and 99.9% significance levels, respectively.

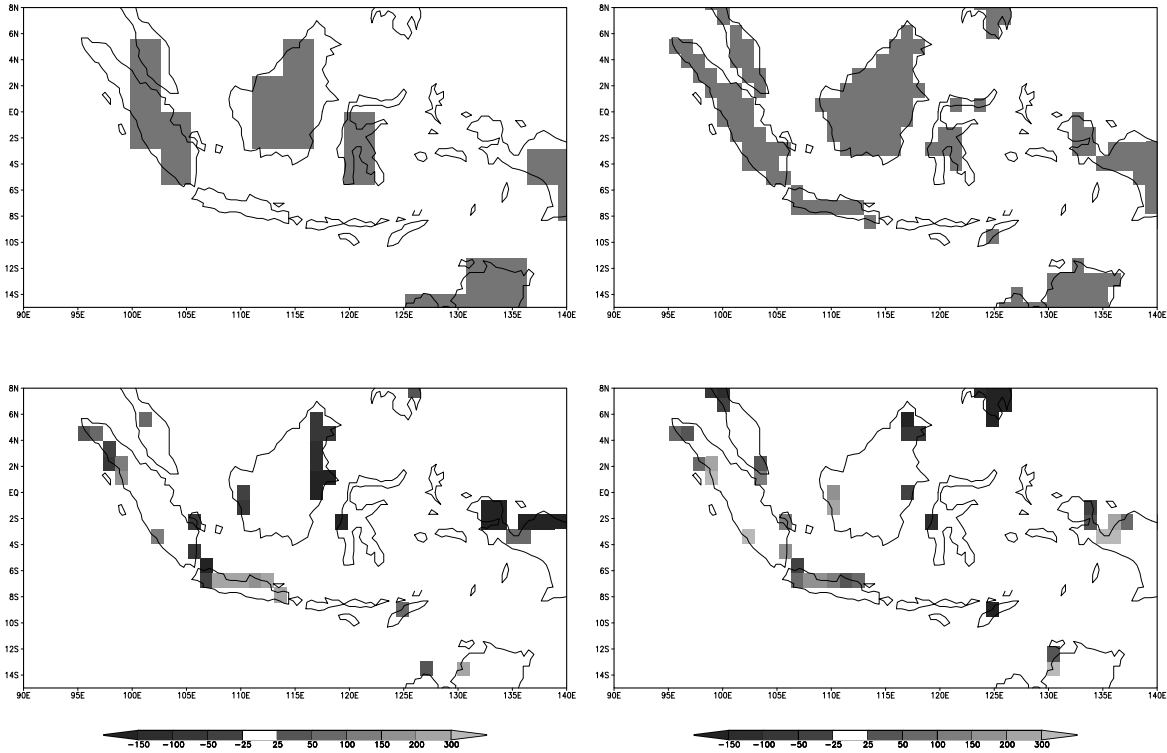|	Region A			Region B			Region C		
	Obs - ERA15	Obs - NRA	Obs - ECHAM	Obs - ERA15	Obs - NRA	Obs - ECHAM	Obs - ERA15	Obs - NRA	Obs - ECHAM
T42	0.78***	0.69***	0.83***	0.24	0.42**	0.22	0.78***	0.88***	0.66**
T106	0.76***	-	0.84***	-0.21	-	0.44**	0.53**	-	0.89***

Figure 14: The land sea mask of the T42 (top left) the T106 (top right) and two examples of calculated errors (mm/month) of newly introduced land grids (top right minus top left figures) by higher resolutions in Jannuary 1979. The bottom left shows errors in T42 and the bottom right in T106.

7   Effects of Land-sea Mask Resolution

The correlation analysis at two different resolutions raises the question of the role of the land-sea mask. Does a higher resolution land mask contribute to higher model skill ? At the T106 resolution there are some additional land areas that do not appear at the T42 resolution. This section focuses on the effect of these additional land grid cells on rainfall errors. The analysis below is restricted to ECHAM4 results, since only ECHAM4 has two independent simulations at two resolutions.

Fig. 14 illustrates the land-sea distribution at both resolutions. Even at the T106 resolution, the model cannot represent some small islands or even the correct shape of a big island such as Sulawesi. The rainfall for those additional land points will be compared to observations at T106, and then the differences will be analyzed. The following section describes as an example the rainfall error at two resolutions in January 1979 for the additional grid cells. We study the statistics of the errors by a scatter plot and frequency distribution diagram.

Fig. 15 shows a scatter plot of errors at both resolutions from ECHAM4. This plot indicates the difference between the newly introduced land points at T106 and the corresponding grid
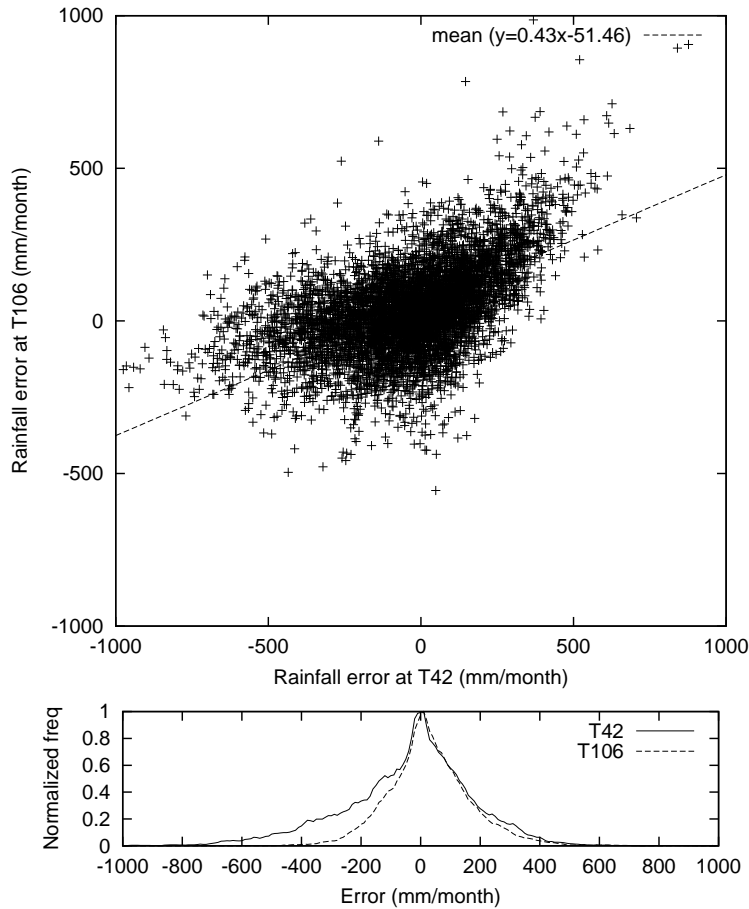
Figure 15: Scatter plots of error distributions by ECHAM4 in two different resolutions of newly introduced land grids. The plots show cases of all errors in 120 months (1979-1988). The bottom part illustrates the normalized frequency distributions of those errors.

points at T42. Although there is no significant shift of peaks or medians between the two curves, the frequency distribution at T42 is broader than that at T106. Thus, there are more underestimations at T42 than at T106 and a more coherent result at T106. Other statistical measures are the mean error and the root mean square (RMS) error values. A greater RMS error at T42 is seen in Fig. 15, where the frequency distribution of T42 is skewed toward the negative side. Overall, the introduction of a new land-sea mask at the higher resolution improves the model performance. *Lal et al.* (1997) found that ECHAM simulation at T106 captures both the spatial and temporal characteristics of the Indian monsoon climatology better than the T42 and produces less erroneous diurnal and seasonal cycles of area-averaged surface air temperature. *Stendel and Roeckner* (1998) studied the influence of horizontal resolutions on ECHAM4 model simulations, and found a more vigorous tropical convection at higher resolution and that a higher resolution model has a positive impact on regional rainfall patterns, which are affected by the

orography. With regard to the rainfall simulated by ECHAM, *May and Roeckner* (2001) found that the resolution effect is particularly strong over the tropical oceans with sharper gradients between wet and dry areas as a result of enhanced convection at T106 in comparison to T42.

8   Concluding Remarks

We have examined the performance of two reanalyses and the ECHAM4 model with regard to rainfall over Indonesia at two different horizontal resolutions. We have introduced a new regionalization method in order to separate climate zones. The analysis focuses on regional, monthly and seasonal means as well as the annual cycle and interannual variability for three such climate regions. The correlation of rainfall to SST variations in the NINO3 region has also been investigated. In addition, the resolution dependence by a changed land sea mask representation at two different resolutions has been addressed.

With the new double correlation method, we have identified three main climate regions each with its own characteristic annual precipitation cycle. These regions simplify the previous regionalization by *Wyrtki* (1956). Many authors use a simple box with definite latitudes and longitudes to designate a climate region. The method presented here is more flexible because the resulting region can have any shape. The regionalization method produces three main climate regions; the southern monsoonal, the northwestern semi-monsoonal and the Moluccan anti-monsoonal.

The simulated rainfall has a seasonal dependence and an ENSO cycle dependence. From the interannual analysis of Region A and C (Fig. 6 and 8), El Niño (La Niña) years are indicated by rainfall index below $-\sigma$ (above $-\sigma$) in SON, except the very weak 1969 El Niño. Thus, the rainfall in SON in either region can be used as an ENSO index. The observation shows that Region A is more sensitive to ENSO (section 4), while Region C has the same length of ENSO impact as Region A and receives the earliest significant ENSO impact (section 6) and there is no ENSO impact in the peak of the wet southeast monsoon. The reanalyses and ECHAM4 simulate variability during ENSO years better when coherent signals appear especially during El Niño years. The study shows better seasonal than monthly model skills. The highest skill occurs in JJA, followed by SON, DJF and MAM. *Haylock and McBride* (2001) showed better predictability of Indonesian rainfall in SON than in DJF. Good skills in JJA promise good ENSO forecast, since the most severe environmental and socio-economic impact of ENSO on Indonesia occurs in SON (*Kirono et al.*, 1999). The study shows the breakdown of the correlation in spring (MAM). Observed SSTs are used as lower boundaries for the reanalyses and very likely the same observed SSTs are used to run the ECHAM4 simulation. Nonetheless the combination of meteorological data and SST yields only a very small correlation for reanalyses in spring (MAM). The observed SST applied to the model even yields an erroneous positive corre-

lation. *Trenberth and Caron* (2000) showed a northward shift of a high correlation area between rainfall over Indonesia and SOI in MAM, whereas in other seasons the Maritime Continent is covered by strong correlations.

Indonesia, except Region B experiences consistent ENSO related rainfall anomalies. These results are in agreement with the results of *Ropelewski and Halpert* (1987, 1989); *Halpert and Ropelewski* (1992). The present study not only gives similar rainfall-anomaly maps as shown by these authors, but also the seasonal march of impact received in each region. Southern Indonesia or Region A is the most El Niño sensitive region. While Region C, which is located in the Indonesian throughflow region, is also an ENSO sensitive region, where the throughflow variation itself is also affected by ENSO (*Meyers*, 1996). This study could be extended with ERA40 (*Simmons and Gibson*, 2000) and the whole NRA40.

Acknowledgements

References

Annamalai, H., J. M. Slingo, K. R. Sperber, and K. Hodges, 1999: The Mean evolution and variability of the Asian summer monsoon Comparison of ECMWF and NCEP-NCAR re-analyses., *Mon. Wea. Rev.*, **127**, 1157–1186.

Asnani, G. C., 1993: *Tropical Meteorology*, vol. 1, Asnani, 603 pp.

Barnett, T. P., K. Arpe, L. Bengtsson, M. Ji, and A. Kumar, 1997: Potential predictability and AMIP implications of midlatitude climate variability in two general circulation models., *J. Climate*, **10**, 2321–2329.

Barnston, A. G., H. M. van den Dool, S. E. Zebiak, T. P. Barnett, M. Ji, D. R. Rodenhuis, M. A. Cane, A. Leetmaa, N. E. Graham, C. R. Ropelewski, V. E. Kousky, E. A. O'Lenic, and R. E. Livezey, 1994: Long-lead seasonal forecasts - Where do we stand?, *Bull. Amer. Meteor. Soc.*, **75**, 2097–2114.

Barnston, A. G., M. H. Glantz, and Y. He, 1999: Predictive skill of statistical and dynamical climate models in forecasts of SST during the 1997-98 El Nio episode and the 1998 La Niña onset., *Bull. Amer. Meteor. Soc.*, **80**, 217–244.

Berlage, H. P., 1927: East-monsoon forecasting in Java., *Verhandelingen 20*, Koninklijk Magnetisch en Meteorologisch Observatorium te Batavia, Magnetic Meteorology Observation. Batavia, Indonesia, 42 pp.

Braak, C., 1919: Atmospheric variations of short and long duration in the Malay Archipelago., *Verhandelingen 5*, Koninklijk Magnetisch en Meteorologisch Observatorium te Batavia, Magnetic Meteorology Observation. Batavia, Indonesia, 57 pp.

Cheang, B. K., 1987: Short- and long- range monsoon prediction in Southeast Asia. in, *Monsoons.* (Eds.), Fein, J. S., and P. L. Stephens, John Wiley and Sons, Wiley Interscience Publication, 579-606 pp.

Chen, W. Y., and H. M. van den Dool, 1997: Atmospheric predictability of seasonal, annual and decadal climate means and the role of the ENSO cycle: a model study., *J. Climate*, **10**, 1236–1254.

Davidson, N. E., 1984: Short-term fluctuations in the Australian monsoon during winter Monex., *Mon. Wea. Rev.*, **112**, 1697–1708.

Davidson, N. E., J. L. McBride, and B. J. McAvaney, 1984: Divergent circulations during the onset of the 1978-79 Australian monsoon., *Mon. Wea. Rev.*, **112**, 1684–1696.

Gates, W. L., 1992: AMIP: The Atmospheric Model Intercomparison Project., *Bull. Amer. Meteor. Soc.*, **73**, 1962–1970.

Gates, W. L., J. S. Boyle, C. Covey, C. G. Dease, C. M. Doutriaux, R. S. Drach, M. Fiorino, P. J. Gleckler, J. J. Hnilo, S. M. Marlais, T. J. Phillips, G. L. Potter, B. D. Santer, K. R. Sperber, K. E. Taylor, and D. N. Williams, 1999: An overview of the results of the Atmospheric Model Intercomparison Project (AMIP I)., *Bull. Amer. Meteor. Soc.*, **80**, 29–56.

Gibson, J. K., P. Kallberg, S. Uppala, A. Hernandez, A. Nomura, and E. Serrano, 1997: The ECMWF Re-Analysis (ERA) 1. ERA Description., *ECMWF Reanalysis Project Series 1*, ECMWF, [Available from the European Centre for Medium-range Weather Forecasts, Reading, UK], 71 pp.

Goddard, L., S. J. Mason, S. E. Zebiak, C. F. Ropelowski, R. Basher, and M. A. Cane, 2000: Current approaches to seasonal to interannual climate predictions., *(IRI) tech. report 00-01*, International Research Inst., 62 pp.

Gutman, G., I. Csiszar, and P. Romanov, 2000: Using NOAA/AVHRR products to monitor El Niño impacts: focus on Indonesia in 1997-98., *Bull. Amer. Meteor. Soc.*, **81**, 1189–1205.

Halpert, M. S., and C. F. Ropelewski, 1992: Temperature patterns associated with the Southern Oscillation., *J. Climate*, **5**, 577–593.

Haylock, M., and J. L. McBride, 2001: Spatial coherence and predictability of Indonesian wet season rainfall., *J. Climate*, **14**, 3882–3887.

Janowiak, J., A. Gruber, C. R. Kondragunta, R. E. Livezey, and G. J. Huffman, 1998: A comparison of the NCEP NCAR reanalysis rainfall and the GPCP rain gauge-satellite combined dataset with observational error considerations, *J. Climate*, **11**, 2960–2979.

Kalnay, E., M. Kanamitsu, R. Kistler, W. Collins, D. Deaven, L. Gandin, M. Iredell, S. Saha, G. White, J. Woollen, Y. Zhu, M. Chelliah, W. Ebisuza, W. Higgins, J. Janowiak, K. C. Mo, C. Ropelewski, J. Wang, A. Leetmaa, R.Reynolds, R. Jenne, and D. Joseph, 1996: The NCEP/NCAR 40-year reanalysis project., *Bull. Amer. Meteor. Soc.*, **77**, 437 – 471.

Kirono, D. G. C., N. J. Tapper, and J. L. McBride, 1999: Documenting Indonesian rainfall in the 1997/1998 El Niño event, *Phys. Geography*, **20**, 422–435.

Lal, M., U. Cubasch, J. Perlwitz, and J. Waszkewitz, 1997: Simulation of the Indian monsoon climatology in ECHAM3 climate model: sensitivity to horizontal resolution, *Int. J. Climatol.*, **17**, 847–858.

Landman, W., and S. J. Mason, 1999: Operational prediction of South African rainfall using canonical correlation analysis., *Int. J. Climatol.*, **19**, 1073–1090.

Lau, N. G., and M. J. Nath, 2000: Impact of ENSO on the variability of the Asian-Australian monsoons as simulated in GCM experiments., *J. Climate*, **13**, 4287 – 4308.

May, W., and E. Roeckner, 2001: A time-slice experiment with the ECHAM4 AGCM at high resolution: the impact of horizontal resolution on annual mean climate change., *Clim. Dyn.*, **17**, 407–420.

Meyers, G., 1996: Variation of the Indonesian throughflow and the El Niño-Southern Oscillation., *J. Geophys. Res.*, **101**, 12,255–12,263.

Moron, V., A. Navarra, M. N. Ward, and E. Roeckner, 1998: Skill and reproducibility of seasonal rainfall patterns in the tropics in ECHAM-4 GCM simulations with prescribed SST., *Clim. Dyn.*, **14**, 83–100.

Newman, M., P. D. Sardeshmukh, and J. W. Bergman, 2000: An assessment of the NCEP, NASA, and ECMWF reanalyses over the tropical west Pacific Warm Pool., *Bull. Amer. Meteor. Soc.*, **81**, 41–48.

Nicholls, N., 1981: Air-sea interaction and the possibility of long-range weather prediction in the Indonesian archipelago., *Mon. Wea. Rev.*, **109**, 2345–2443.

Nicholls, N., 1984: The Southern Oscillation and Indonesia sea surface temperature., *Mon. Wea. Rev.*, **112**, 424–432.

Philander, S. G. H., 1989: *El Niño, La Niña, and the Southern Oscillation.*, vol. 46 of *International Geophysical Series*, Academic Press, 289 pp.

Ramage, C., 1971: *Monsoon Meteorology*, Academic Press, 296 pp.

Rayner, N. A., E. B. Horton, D. E. Parker, C. K. Folland, and R. B. Hackett, 1996: Version 2.2 of the global sea-ice and sea surface temperature data set, 1903-1994., *Tech. Note CRTN74*, Climate Research, 35 pp.

Reesinck, J. J. M., 1952: Some remarks on monsoon forecasting for Java., *Verhandelingen 44*, Kementrian Perhubungan Lembaga Meteorologi dan Geofisika, Jakarta, Indonesia, 22 pp.

Roeckner, E., K. Arpe, L. Bengston, M. Christoph, M. Claussen, L. Dumenil, M. Esch, M. Giorgetta, U. Schlese, and U. Schulzweida, 1996a: The atmospheric general circulation model ECHAM-4: Model description and simulation of present-day climate., *MPI Report 218*, [Available from Max Planck-Institut für Meteorologie, Bundesstr. 55, D-20146, Hamburg, Germany.], 90 pp.

Roeckner, E., J. M. Oberhuber, A. Bacher, M. Christoph, and I. Kirchner, 1996b: ENSO variability and atmospheric response in a global coupled atmosphere-ocean GCM., *Clim. Dyn.*, **12**, 737–754.

Ropelewski, C., and M. S. Halpert, 1989: Rainfall patterns associated with the high index phase of the Southern Oscillation., *J. Climate*, **2**, 268–284.

Ropelewski, C. F., and M. S. Halpert, 1987: Global and regional scale rainfall patterns associated with the El Niño Southern Oscillation (ENSO)., *Mon. Wea. Rev.*, **115**, 1606–1626.

Schell, I. I., 1947: *Dynamic persistence and its applications to long-range forecasting.*, vol. 8, Harvard Meteorological Studies, Blue Hill Observatory, Milton, MA, 80 pp.

Simmons, A. J., and J. K. Gibson, 2000: The ERA-40 Project Plan., *ERA-40 Project Report Series 1*, ECMWF, [Available from the European Centre for Medium-range Weather Forecasts, Reading, UK], 62 pp.

Stendel, M., and K. Arpe, 1997: Evaluation of the hydrological cycle in reanalyses and observations., *MPI Report 228*, [Available from Max-Planck-Institut für Meteorologie, Bundesstrasse 55, 20146 Hamburg, Germany.], 52 pp.

Stendel, M., and E. Roeckner, 1998: Impacts of horizontal resolution on simulated climate statistics in ECHAM4., *MPI Report 253*, [Available from Max Planck-Institut für Meteorologie, Bundesstr. 55, D-20146, Hamburg, Germany.], 57 pp.

Trenberth, K., and J. M. Caron, 2000: The Southern Oscillation revisited: sea level pressure, surface temperature, and precipitation, *J. Climate*, **13**, 4358–4365.

Vose, R. S., R. L. Schmoyer, P. M. Steurer, T. C. Peterson, R. Heim, T. R. Karl, and J. K. Eischeid, 1992: The Global Historical Climatology Network: Long-term monthly temperature, precipitation, sea level pressure, and station pressure data., *ORNL/CDIAC-53 NDP-041*, 325 pp.

WCRP, 1990: Global Rainfall Climatology Project: Implementation and data management plan., *Tech. Rep. WMO/TD-No. 367*, World Climate Research Programme, WMO, Geneva, Switzerland, 47 pp.

Wyrtki, K., 1956: The Rainfall over the Indonesian waters., *Verhandelingen 49*, Kementrian Perhubungan Lembaga Meteorologi dan Geofisika, Jakarta, Indonesia, 24 pp.

MPI-Report-Reference:	*Reprinted in
Report 1 - 290	Please order the reference list from MPI for Meteorology, Hamburg

Report No. 290
June 1999

A nonlinear impulse response model of the coupled carbon cycle-ocean-atmosphere climate system
Georg Hooss, Reinhard Voss, Klaus Hasselmann, Ernst Maier-Reimer, Fortunat Joos

Report No. 291
June 1999

Rapid algorithms for plane-parallel radiative transfer calculations
Vassili Prigarin

Report No. 292
June 1999

Oceanic Control of Decadal North Atlantic Sea Level Pressure Variability in Winter
Mojib Latif, Klaus Arpe, Erich Roeckner
* Geophysical Research Letters, 1999 (submitted)

Report No. 293
July 1999

A process-based, climate-sensitive model to derive methane emissions from natural wetlands:
Application to 5 wetland sites, sensitivity to model parameters and climate
Bernadette P. Walter, Martin Heimann
* Global Biogeochemical Cycles, 1999 (submitted)

Report No. 294
August 1999

Possible Changes of $\delta^{18}O$ in Precipitation Caused by a Meltwater Event in the North Atlantic
Martin Werner, Uwe Mikolajewicz, Georg Hoffmann, Martin Heimann
* Journal of Geophysical Research - Atmospheres, 105, D8, 10161-10167, 2000

Report No. 295
August 1999

Borehole versus Isotope Temperatures on Greenland:
Seasonality Does Matter
Martin Werner, Uwe Mikolajewicz, Martin Heimann, Georg Hoffmann
* Geophysical Research Letters, 27, 5, 723-726, 2000

Report No. 296
August 1999

Numerical Modelling of Regional Scale Transport and Photochemistry directly together with Meteorological Processes
Bärbel Langmann
* Atmospheric Environment, 34, 3585-3598, 2000

Report No. 297
August 1999

The impact of two different land-surface coupling techniques in a single column version of the ECHAM4 atmospheric model
Jan-Peter Schulz, Lydia Dümenil, Jan Polcher
* Journal of Applied Meteorology, 40, 642-663, 2001

Report No. 298
September 1999

Long-term climate changes due to increased CO_2 concentration in the coupled atmosphere-ocean general circulation model ECHAM3/LSG
Reinhard Voss, Uwe Mikolajewicz
* Climate Dynamics, 17, 45-60, 2001

Report No. 299
October 1999

Tropical Stabilisation of the Thermohaline Circulation in a Greenhouse Warming Simulation
Mojib Latif, Erich Roeckner
* Journal of Climate, 1999 (submitted)

Report No. 300
October 1999

Impact of Global Warming on the Asian Winter Monsoon in a Coupled GCM
Zeng-Zhen Hu, Lennart Bengtsson, Klaus Arpe
* Journal of Geophysical Research-Atmosphere, 105, D4, 4607-4624, 2000

Report No. 301
December 1999

Impacts of Deforestation and Afforestation in the Mediterranean Region as Simulated by the MPI Atmospheric GCM
Lydia Dümenil Gates, Stefan Ließ

Report No. 302
December 1999

Dynamical and Cloud-Radiation Feedbacks in El Niño and Greenhouse Warming
Fei-Fei Jin, Zeng-Zhen Hu, Mojib Latif, Lennart Bengtsson, Erich Roeckner
* Geophysical Research Letter, 28, 8, 1539-1542, 2001

MPI-Report-Reference: *Reprinted in

Report 1 - 290 Please order the reference list from MPI for Meteorology, Hamburg

Report No. 303
December 1999
The leading variability mode of the coupled troposphere-stratosphere winter circulation in different climate regimes
Judith Perlwitz, Hans-F. Graf, Reinhard Voss
* Journal of Geophysical Research, 105, 6915-6926, 2000

Report No. 304
January 2000
Generation of SST anomalies in the midlatitudes
Dietmar Dommenget, Mojib Latif
* Journal of Climate, 1999 (submitted)

Report No. 305
June 2000
Tropical Pacific/Atlantic Ocean Interactions at Multi-Decadal Time Scales
Mojib Latif
* Geophysical Research Letters, 28,3,539-542,2001

Report No. 306
June 2000
On the Interpretation of Climate Change in the Tropical Pacific
Mojib Latif
* Journal of Climate, 2000 (submitted)

Report No. 307
June 2000
Observed historical discharge data from major rivers for climate model validation
Lydia Dümenil Gates, Stefan Hagemann, Claudia Golz

Report No. 308
July 2000
Atmospheric Correction of Colour Images of Case I Waters - a Review of Case II Waters - a Review
D. Pozdnyakov, S. Bakan, H. Grassl
* Remote Sensing of Environment, 2000 (submitted)

Report No. 309
August 2000
A Cautionary Note on the Interpretation of EOFs
Dietmar Dommenget, Mojib Latif
* Journal of Climate, 2000 (submitted)

Report No. 310
September 2000
Midlatitude Forcing Mechanisms for Glacier Mass Balance Investigated Using General Circulation Models
Bernhard K. Reichert, Lennart Bengtsson, Johannes Oerlemans
* Journal of Climate, 2000 (accepted)

Report No. 311
October 2000
The impact of a downslope water-transport parameterization in a global ocean general circulation model
Stephanie Legutke, Ernst Maier-Reimer

Report No. 312
November 2000
The Hamburg Ocean-Atmosphere Parameters and Fluxes from Satellite Data (HOAPS): A Climatological Atlas of Satellite-Derived Air-Sea-Interaction Parameters over the Oceans
Hartmut Graßl, Volker Jost, Ramesh Kumar, Jörg Schulz, Peter Bauer, Peter Schlüssel

Report No. 313
December 2000
Secular trends in daily precipitation characteristics: greenhouse gas simulation with a coupled AOGCM
Vladimir Semenov, Lennart Bengtsson

Report No. 314
December 2000
Estimation of the error due to operator splitting for micro-physical-multiphase chemical systems in meso-scale air quality models
Frank Müller
* Atmospheric Environment, 2000 (submitted)

Report No. 315
January 2001
Sensitivity of global climate to the detrimental impact of smoke on rain clouds (only available as pdf-file on the web)
Hans-F. Graf, Daniel Rosenfeld, Frank J. Nober

Report No. 316
March 2001
Lake Parameterization for Climate Models
Ben-Jei Tsuang, Chia-Ying Tu, Klaus Arpe

Report No. 318
March 2001
On North Pacific Climate Variability
Mojib Latif
* Journal of Climate, 2001 (submitted)

MPI-Report-Reference: *Reprinted in

Report 1 - 290   Please order the reference list from MPI for Meteorology, Hamburg

Report No. 319   **The Madden-Julian Oscillation in the ECHAM4 / OPYC3 CGCM**
March 2001   Stefan Liess, Lennart Bengtsson, Klaus Arpe
                            * Climate Dynamics, 2001 (submitted)

Report No. 320   **Simulated Warm Polar Currents during the Middle Permian**
May 2001   A. M. E. Winguth, C. Heinze, J. E. Kutzbach, E. Maier-Reimer,
                            U. Mikolajewicz, D. Rowley, A. Rees, A. M. Ziegler
                            * Paleoceanography, 2001 (submitted)

Report No. 321   **Impact of the Vertical Resolution on the Transport of Passive Tracers**
June 2001   **in the ECHAM4 Model**
                            Christine Land, Johann Feichter, Robert Sausen
                            * Tellus, 2001 (submitted)

Report No. 322   **Summer Session 2000**
August 2001   **Beyond Kyoto: Achieving Sustainable Development**
                            Edited by Hartmut Graßl and Jacques Léonardi

Report No. 323   **An atlas of surface fluxes based on the ECMWF Re-Analysis-**
July 2001   **a climatological dataset to force global ocean general circulation**
                            models
                            Frank Röske

Report No. 324   **Long-range transport and multimedia partitioning of semivolatile**
August 2001   **organic compounds:**
                            A case study on two modern agrochemicals
                            Gerhard Lammel, Johann Feichter, Adrian Leip
                            * Journal of Geophysical Research-Atmospheres, 2001 (submitted)

Report No. 325   **A High Resolution AGCM Study of the El Niño Impact on the North**
August 2001   **Atlantic / European Sector**
                            Ute Merkel, Mojib Latif
                            * Geophysical Research Letters, 2001 (submitted)

Report No. 326   **On dipole-like varibility in the tropical Indian Ocean**
August 2001   Astrid Baquero-Bernal, Mojib Latif
                            * Journal of Climate, 2001 (submitted)

Report No. 327   **Global ocean warming tied to anthropogenic forcing**
August 2001   Berhard K. Reichert, Reiner Schnur, Lennart Bengtsson
                            * Geophysical Research Letters, 2001 (submitted)

Report No. 328   **Natural Climate Variability as Indicated by Glaciers and Implications**
August 2001   **for Climate Change: A Modeling Study**
                            Bernhard K. Reichert, Lennart Bengtsson, Johannes Oerlemans
                            * Journal of Climate, 2001 (submitted)

Report No. 329   **Vegetation Feedback on Sahelian Rainfall Variability in a Coupled**
August 2001   **Climate Land-Vegetation Model**
                            K.-G. Schnitzler, W. Knorr, M. Latif, J.Bader, N.Zeng
                            Geophysical Research Letters, 2001 (submitted)

Report No. 330   **Structural Changes of Climate Variability** (only available as pdf-file on the web)
August 2001   H.-F.Graf, J. M. Castanheira
                            Journal of Geophysical Research -Atmospheres, 2001 (submitted)

Report No. 331   **North Pacific - North Atlantic relationships under stratospheric**
August 2001   **control?** (only available as pdf-file on the web)
                            H.-F.Graf, J. M. Castanheira
                            Journal of Geophysical Research -Atmospheres, 2001 (submitted)

Report No. 332   **Using a Physical Reference Frame to study Global Circulation**
September 2001   **Variability** (only available as pdf-file on the web)
                            H.-F.Graf, J. M. Castanheira, C.C. DaCamara, A.Rocha

MPI-Report-Reference: *Reprinted in

Report 1 - 290   Please order the reference list from MPI for Meteorology, Hamburg

Journal of Atmospheric Sciences, 2001 (in press)

Report No. 333
November 2001
**Stratospheric Response to Global Warming in the Northern
Hemisphere Winter**
Zeng-Zhen Hu

Report No. 334
October 2001
**On the Role of European and Non-European Emission Sources
for the Budgets of Trace Compounds over Europe**
Martin G. Schultz, Johann Feichter, Stefan Bauer, Andreas Volz-Thomas

Report No. 335
November 2001
**Slowly Degradable Organics in the Atmospheric Environment
and Air-Sea Exchange**
Gerhard Lammel

Report No. 336
January 2002
**An Improved Land Surface Parameter Dataset for Global
and Regional Climate Models**
Stefan Hagemann

Report No. 337
May 2002
**Lidar intercomparisons on algorithm and system level
in the frame of EARLINET**
Volker Matthias, J. Bösenberg, H. Linné, V. Matthias, C. Böckmann,
M. Wiegner, G. Pappalardo, A. Amodeo, V. Amiridis, D. Balis, C. Zerefos,
A. Ansmann, I. Mattis, U. Wandinger, A. Boselli, X. Wang, A. Chaykovski,
V. Shcherbakov, G. Chourdakis, A. Papayannis, A. Comeron,
F. Rocadenbosch, A. Delaval, J. Pelon, L. Sauvage, F. DeTomasi,
R. M. Perrone, R. Eixmann, J. Schneider, M. Frioud, R. Matthey, A. Hagard,
R. Persson, M. Iarlori, V. Rizi, L. Konguem, S. Kreipl, G. Larchevêque,
V. Simeonov, J. A. Rodriguez, D. P. Resendes, R. Schumacher

Report No. 338
June 2002
**Intercomparison of water and energy budgets simulated by regional
climate models applied over Europe**
Stefan Hagemann, Bennert Machenhauer, Ole Bøssing Christensen,
Michel Déqué, Daniela Jacob, Richard Jones, Pier Luigi Vidale

Report No. 339
September 2002
**Modelling the wintertime response to upper tropospheric and lower
stratospheric ozone anomalies over the North Atlantic and Europe**
Ingo Kirchner, Dieter Peters

Report No. 340
November 2002
**On the determination of atmospheric water vapour from GPS
measurements**
Stefan Hagemann, Lennart Bengtsson, Gerd Gendt

Report No. 341
November 2002
The impact of international climate policy on Indonesia
Armi Susandi, Richard S.J. Tol

Report No. 342
December 2002
**Indonesian smoke aerosols from peat fires and the contribution from
volcanic sulfur emissions** (only available as pdf-file on the web)
Bärbel Langmann, Hans F. Graf

Report No. 343
January 2003
Modes of the wintertime Arctic temperature variability
Vladimir A. Semenov, Lennart Bengtsson

Report No. 344
February 2003
**Indicators for persistence and long-range transport potential as
derived from multicompartment chemistry-transport modelling**
Adrian Leip, Gerhard Lammel

Report No. 345
February 2003
The early century warming in the Arctic – A possible mechanism
Lennart Bengtsson, Vladimir A. Semenov, Ola Johannessen